AD-A108 013 AIR FORCE INST OF TECH WRIGHT-PATTERSON AFB OH F/G 17/9
GUST FRONT RECOGNITION USING A SINGLE-DOPPLER RADAR.(U)
1979 M W MADER
UNCLASSIFIED AFIT-CI-79-283T-S NL

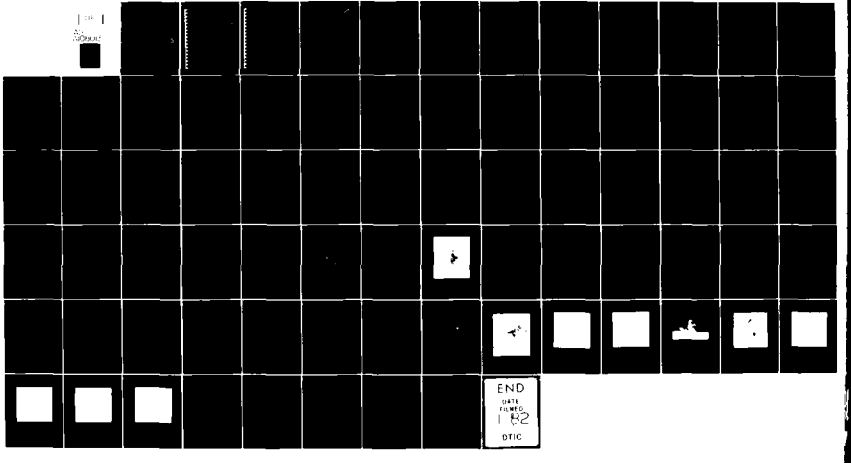

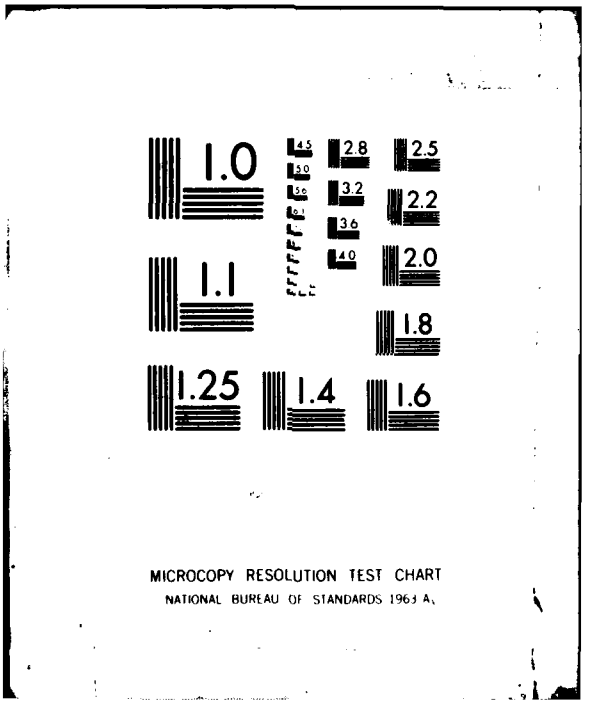
1.0
1.1
1.25
1.4
1.6
1.8
2.0
2.2
2.5
2.8
3.2
3.6
4.0
MICROCOPY RESOLUTION TEST CHART
NATIONAL BUREAU OF STANDARDS 1963 A

UNCLASS

SECURITY CLASSIFICATION OF THIS PAGE (When Data Entered)

(14) AFIT-CI-

REPORT DOCUMENTATION PAGE

READ INSTRUCTIONS BEFORE COMPLETING FORM

1. REPORT NUMBER: 79-283T-S (6)	2. GOVT ACCESSION NO.: AD A108013
3. RECIPIENT'S CATALOG NUMBER	
4. TITLE (and Subtitle): Gust Front Recognition Using a Single-Doppler Radar.	5. TYPE OF REPORT & PERIOD COVERED: THESIS/DISSERTATION
	6. PERFORMING ORG. REPORT NUMBER
7. AUTHOR(s): Michael William Mader (10)	8. CONTRACT OR GRANT NUMBER(s): (9) masters thesis
9. PERFORMING ORGANIZATION NAME AND ADDRESS: AFIT STUDENT AT: Univ of Oklahoma	10. PROGRAM ELEMENT, PROJECT, TASK AREA & WORK UNIT NUMBERS: (11)
11. CONTROLLING OFFICE NAME AND ADDRESS: AFIT/NR WPAFB OH 45433 (12)	12. REPORT DATE: 1979
	13. NUMBER OF PAGES: 71
14. MONITORING AGENCY NAME & ADDRESS (if different from Controlling Office)	15. SECURITY CLASS. (of this report): UNCLASS
	15a. DECLASSIFICATION/DOWNGRADING SCHEDULE

16. DISTRIBUTION STATEMENT (of this Report)

APPROVED FOR PUBLIC RELEASE; DISTRIBUTION UNLIMITED

17. DISTRIBUTION STATEMENT (of the abstract entered in Block 20, if different from Report)

23 NOV 1981

18. SUPPLEMENTARY NOTES

APPROVED FOR PUBLIC RELEASE: IAW AFR 190-17

Fredric C. Lynch
FREDRIC C. LYNCH, Major, USAF
Director of Public Affairs
Air Force Institute of Technology (ATC)
Wright-Patterson AFB, OH 45433

19. KEY WORDS (Continue on reverse side if necessary and identify by block number)

20. ABSTRACT (Continue on reverse side if necessary and identify by block number)

ATTACHED

AD A108013

LEVEL II

DTIC ELECTE DEC 2 1981 D H

DTIC FILE COPY

DD FORM 1 JAN 73 1473 EDITION OF 1 NOV 65 IS OBSOLETE

UNCLASS 01200

SECURITY CLASSIFICATION OF THIS PAGE (When Data Entered)

81 11 30 02

ABSTRACT

Author : Michael W. Mader

Title : Gust Front Recognition Using a Single-Doppler Radar

Military Rank : Captain

Service Branch : USAF

Date : 1979

Number of Pages : 71

Degree Awarded : Master of Science in Meteorology

Name of Institution : University of Oklahoma

This research developed from an Air Force interest in using the Doppler radar to forecast strong low-level outflow from thunderstorms. Much of the data were obtained during the author's participation in the Joint Doppler Operational Project (JDOP) during the spring of 1978.

A dual-Dopper analysis ~~(Brandes, 1975)~~ of a squall-line on 3 May 1977 yielded a three-dimensional wind field within what was considered a "typical" squall-line. This wind field was highly divergent near the surface in the area of the downdraft. Directly above this divergent flow, at a height of 3 to 6 km, the flow became highly convergent, with dry air entrainment observed along the backside of the storm. The wind field above 6 km showed only small areas of weak convergence. This lead to the conclusion that the mid-level (3 to 6 km) air was the main source of the downdraft air responsible for the strong surface outflow. A θ_w analysis helped verify this conclusion.

Based on the idea that the mid-level convergence is an indication of a strong downdraft, the dual-Doppler wind field was converted to radial wind fields as would be viewed from various angles by a single-Doppler radar. To be able to use this idea in real-time operations, convergence values along each radial were computed relative to the azimuth of the radar and direction of storm motion. — next page

To further illustrate the possible use of this convergence signature, single-Doppler data of three thunderstorms known to have produced strong surface winds were examined. In all three cases, a strong convergent boundary was present in the mid-levels of the storm.

This research indicated mid-level convergence may be a characteristic of thunderstorms which produce a strong downdraft and subsequently strong outflow. By indentifying such a feature in the mid-levels of the storm, the problems of warning on storms located at a distance in excess of 100 km or storms with a gust front out ahead of the precipitation would be eliminated. The author believes that experienced forecasters with a thorough understanding of thunderstorm dynamics can use this convergence boundary as a forecasting tool when using a single-Doppler radar to warn on thunderstorm induced high winds.

PRIMARY REFERENCES

Bonewitz, J.D., 1978: Development of Doppler radar techniques for severe thunderstorm wind advisories. Master's Thesis, University of Oklahoma, 69 pp.

Brandes, E.A., 1975: Severe thunderstorm flow characteristics revealed by dual-Doppler observations: 6 June 1974. Preprints, 9th Conf. on Severe Local Storms, Boston, Amer. Meteor. Soc., 85-90.

_____, 1976: Gust front evolution in severe thunderstorms: Preliminary investigation with Doppler radar. Preprints, 7th Conf. on Aerospace and Aeronautical Meteor., Melbourne, Amer. Meteor. Soc., 56-61.

Goff, R.C., 1976: Vertical structure of thunderstorm outflow. Mon. Wea. Rev., 104, 1430-1440.

Kropfli, R.A., and L.J. Miller, 1975: Kinematic structure and flux quantities in a convective storm from dual-Doppler radar observations. J. Appl. Meteor., 33, 520-529.

Lemon, L.R., R.J. Donaldson, Jr., D.W. Burgess, and R.A. Brown, 1977: Doppler radar application to severe thunderstorm study and potential real-time warning. Bull. Amer. Meteor. Soc., 58, 1187-1193.

THE UNIVERSITY OF OKLAHOMA

GRADUATE COLLEGE

GUST FRONT RECOGNITION USING A SINGLE-DOPPLER RADAR

A THESIS

SUBMITTED TO THE GRADUATE FACULTY

in partial fulfillment of the requirements for the

degree of

MASTER OF SCIENCE IN METEOROLOGY

By

MICHAEL WILLIAM MADER

Norman, Oklahoma

1979

GUST FRONT RECOGNITION USING A

SINGLE-DOPPLER RADAR

A THESIS

APPROVED BY THE DEPARTMENT OF METEOROLOGY

By

James F. Kimpel

John M. McGuirk

Ronnie L. Whitney

Don W. Burgess

ACKNOWLEDGEMENTS

The completion of this research would not have been possible without the cooperation of many persons. The author wishes to express his appreciation to Dr. James F. Kimpel, Dr. John McCarthy (both of the University of Oklahoma), and Dr. Ronnie L. Alberty (National Severe Storms Laboratory, NSSL) for their helpful criticism and recommendations. Special thanks go to Don W. Burgess (NSSL) for his continual support and suggestions throughout the completion of this research.

The data used for this study was provided by NSSL and the help of all staff members has been appreciated. Edward A. Brandes, Stephan P. Nelson, and Leroy Fortner were all extremely helpful in their computer programming assistance. Thanks go to Jennifer Moore and Chuck Clark for drafting and photographing the figures, and Evelyn Horwitz for typing this manuscript.

To my wife, Kathy, go much more than the usual thanks for her cooperation and patience. She was always there to pick me up when I was down and showed that she really believed in me.

TABLE OF CONTENTS

LIST OF FIGURES

LIST OF TABLES

ABSTRACT

Author : Michael W. Mader

Title : Gust Front Recognition Using a Single-Doppler Radar

Military Rank : Captain

Service Branch : USAF

Date : 1979

Number of Pages : 71

Degree Awarded : Master of Science in Meteorology

Name of Institution : University of Oklahoma

This research developed from an Air Force interest in using the Doppler radar to forecast strong low-level outflow from thunderstorms. Much of the data were obtained during the author's participation in the Joint Doppler Operational Project (JDOP) during the spring of 1978.

A dual-Dopper analysis (Brandes, 1975) of a squall-line on 3 May 1977 yielded a three-dimensional wind field within what was considered a "typical" squall-line. This wind field was highly divergent near the surface in the area of the downdraft. Directly above this divergent flow, at a height of 3 to 6 km, the flow became highly convergent, with dry air entrainment observed along the backside of the storm. The wind field above 6 km showed only small areas of weak convergence. This lead to the conclusion that the mid-level (3 to 6 km) air was the main source of the downdraft air responsible for the strong surface outflow. A Θ_w analysis helped verify this conclusion.

Based on the idea that the mid-level convergence is an indication of a strong downdraft, the dual-Doppler wind field was converted to radial wind fields as would be viewed from various angles by a single-Doppler radar. To be able to use this idea in real-time operations, convergence values along each radial were computed relative to the azimuth of the radar and direction of storm motion.

To further illustrate the possible use of this convergence signature, single-Doppler data of three thunderstorms known to have produced strong surface winds were examined. In all three cases, a strong convergent boundary was present in the mid-levels of the storm.

This research indicated mid-level convergence may be a characteristic of thunderstorms which produce a strong downdraft and subsequently strong outflow. By indentifying such a feature in the mid-levels of the storm, the problems of warning on storms located at a distance in excess of 100 km or storms with a gust front out ahead of the precipitation would be eliminated. The author believes that experienced forecasters with a thorough understanding of thunderstorm dynamics can use this convergence boundary as a forecasting tool when using a single-Doppler radar to warn on thunderstorm induced high winds.

PRIMARY REFERENCES

Bonewitz, J.D., 1978: Development of Doppler radar techniques for severe thunderstorm wind advisories. Master's Thesis, University of Oklahoma, 69 pp.

Brandes, E.A., 1975: Severe thunderstorm flow characteristics revealed by dual-Doppler observations: 6 June 1974. Preprints, 9th Conf. on Severe Local Storms, Boston, Amer. Meteor. Soc., 85-90.

_____, 1976: Gust front evolution in severe thunderstorms: Preliminary investigation with Doppler radar. Preprints, 7th Conf. on Aerospace and Aeronautical Meteor., Melbourne, Amer. Meteor. Soc., 56-61.

Goff, R.C., 1976: Vertical structure of thunderstorm outflow. Mon. Wea. Rev., 104, 1430-1440.

Kropfli, R.A., and L.J. Miller, 1975: Kinematic structure and flux quantities in a convective storm from dual-Doppler radar observations. J. Appl. Meteor., 33, 520-529.

Lemon, L.R., R.J. Donaldson, Jr., D.W. Burgess, and R.A. Brown, 1977: Doppler radar application to severe thunderstorm study and potential real-time warning. Bull. Amer. Meteor. Soc., 58, 1187-1193.

GUST FRONT RECOGNITION USING A SINGLE-DOPPLER RADAR

1. INTRODUCTION

Conventional radars have been used to detect severe thunderstorms since the early 1940's. Significant advancements have been made in the understanding of the wind fields within convective storms since the development and use of the Doppler radar in a research mode. To test the feasibility of the Doppler radar in an operational environment, the Joint Doppler Operational Project (JDOP) was formed. This joint agency project* will determine the suitability of the Doppler radar as the next generation radar. A complete explanation of the project and the results from the tests conducted during the springs of 1977 and 1978 are included in JDOP Staff, 1979.

During the JDOP test conducted during the spring of 1978, a team composed of forecasters from AWS, NWS, AFGL, and NSSL used the Norman Doppler radar to issue severe weather advisories to the NWS offices and Air Force Bases in Oklahoma, Northern Texas, Western Arkansas, Southern Kansas, and extreme Southwestern Missouri. Before

*The agencies participating in JDOP include Air Weather Service (AWS), National Weather Service (NWS), Environmental Research Laboratories (ERL), especially the National Severe Storms Laboratory (NSSL), Federal Aviation Administration (FAA), and the Air Force Geophysics Laboratory (AFGL).

the spring operations began, Doppler radar signatures or profiles that would be used as an indicator of severe storms were established. Mesocyclone and tornado vortex wind signatures had been identified (Donaldson, 1970; Burgess, 1976; and Lemon et al., 1977) and used with good success during the two years of the JDOP test. Reflectivity profiles were the main indicator used in identifying large (greater than 3/4 inch) hail producing storms. During spring operations it became apparent that the divergent outflow signature seen near the top of the storm was a good indicator of the strength of the updraft. When high values of divergence were noticed, the storm was considered as one likely to produce hail. Michael R. Snapp, AWS forecaster, is using Doppler data to research this idea further.

There has been great difficulty in discerning a signature for strong straight line winds. The Doppler radar can measure only the displacement of the scatters along the radar beam. Therefore, the wind velocity sampled by a single-Doppler radar is only that component of the true wind which is oriented in the direction that the radar is pointed. During JDOP operations, the magnitude of the radial component of the wind in the lowest kilometer above the ground was used in issuing wind advisories. If the direction of the wind was nearly perpendicular to the radar beam, little evidence of high winds was noted and no advisory was issued. If the storm was located over 100 km away from Norman, no advisory could be issued because the radar beam, even at 0.2° elevation angle, was sampling at a height near 1 km.

While it is very important to AWS to be able to detect a tornado vortex, mesocyclone, or a large hail producing storm, the ability to

identify those storms likely to produce high winds is of equal or even greater importance. Little can be done to avoid tornado or hail damage to the very expensive aircraft parked on an airfield. However, with early warning, damage to aircraft caused by high winds can be prevented. This, coupled with the hazards caused by turbulence and strong wind changes encountered during takeoff and landing, makes being able to forecast strong thunderstorm outflow very important to the Air Force. Although this research was generated by an Air Force interest, it can also benefit the civilian community. The FAA has shown an extreme interest in gust front detection for basically the same reasons as the Air Force. Perhaps the most important aspect of early detection and warning of an approaching gust front is the possible prevention of the loss of lives and the prevention of excessive property damage.

In order to develop a signature or profile usable with the Doppler velocity display, an understanding of the kinematic and dynamic processes occurring within a thunderstorm, producing a gust front, is necessary. The basic air flow in and around a typical mature squall-line is depicted in figure 1. Although it is generally accepted that strong outflow is the result of an intense downdraft, Byers and Braham (1949) proposed the idea that the downdraft is initiated by precipitation drag. That is, large precipitation particles (both rain and hail) act to drag the surrounding air downward as they fall. Byers and Braham (1949) and Fankhauser (1971) suggest that the downdraft is also enhanced by entrainment of mid-tropospheric air into the storm. This entrainment is created when the storm is moving slower than the environment winds at mid-levels. The thunderstorm then acts as an obstacle

to the flow, forcing the air to either flow around the storm or be mixed into the cloud boundary. The cooler, drier air mixing with the mid-levels of the storm acts to evaporate the smaller water droplets. This evaporation process cools the air, making it less bouyant, and causes the downdraft to be enhanced. The horizontal momentum of the ingested air is also partially conserved, and when transported downward to the surface acts to accelerate the outflow ahead of the storm. The convergent boundary that results from the thunderstorm outflow (cold air) and the warm air inflow is what is referred to as the gust front (Brandes, 1976).

Since the gust front is a boundary layer phenomenon, much research has been limited to data obtained at or very near the surface. An added facet to surface data has been the use of instrumented towers. Goff (1976), using data obtained from NSSL's 481 meter instrumented tower on 20 thunderstorm outflow cases, constructed 450 meter time-height cross sections of wind and temperature profiles. Charba (1974) used the NSSL tower and mesonetwork data to profile the three-dimensional wind and thermal field of an intense gust front on 31 May 1969. Barnes (1978) combined surface mesonetwork data with upper air rawinsondes to describe the flow around two severe thunderstorms on 29 and 30 April 1970. Barnes suggests that a downdraft may form on the rear flank of the storm due entirely to evaporative cooling of the mid-tropospheric flow and the conservation of the horizontal momentum. Numerical modeling of thunderstorms has led to limited results in gust front analysis. Mitchell and Hovermale (1977) derived a two-dimensional (x-z) model of a gust front with results that compare well with observed data.

The use of multiple-Doppler data in understanding the dynamics of thunderstorms has affected research operations considerably over the past few years. Most Doppler radar research of thunderstorms (e.g., Armstrong and Donaldson, 1969; Burgess, 1976; and Brown et al., 1978) and thunderstorm outflow (Brandes, 1975, 1976, 1977) have been associated with a mesocyclone. Kropfli and Miller (1975) used dual-Doppler data of a thunderstorm in northeast Colorado to analyze the three-dimensional wind field. This storm exhibited weak cyclonic shear (9×10^{-4} s^{-1}) that never met mesocyclone criteria (Burgess, 1976). The interesting features of this storm are the strong divergent flow at the surface (8×10^{-3} s^{-1}), corresponding to the area of highest reflectivity (40 dBZ), and the convergent flow at 3 km AGL, again corresponding to the area of high reflectivity and area of descending air.

Bonewitz (1978) began research into the area of gust front recognition while participating in the JDOP test in the spring of 1977. By using the single-Doppler (Norman) data of a squall-line on 3 May 1977, Bonewitz showed a very high correlation between the radial wind seen below 1 km by the Doppler radar and the wind observed on the surface at the NSSL mesonetwork sites. Bonewitz concluded that by using a basic trigonometric relationship between the direction of the Doppler radial velocity and an estimation of the direction of the thunderstorm outflow, a good approximation of the magnitude of the horizontal surface wind can be made.

This research herein was a continuation of the work started for the Air Force by Bonewitz. However, this research concentrated more on the mid-levels of the storm, attempting to identify a velocity pattern

that may give an indication of whether a particular thunderstorm will produce strong surface winds. First, a dual-Doppler analysis of a squall-line known to have produced strong surface winds was performed to obtain an approximation of the three-dimensional wind field. Using this wind field, a conversion was made back to radial winds that would be seen by a Doppler radar located at various positions around the storm. To illustrate the usefulness of the results, three cases of thunderstorms which occurred during JDOP operations in 1978 were examined.

2. SEARCH FOR A WIND SIGNATURE

Attempts were made to examine all the 1978 single-Doppler velocity data obtained during JDOP operations and to use a statistical comparison to see if any distinguishing feature would identify a particular storm as one likely to produce strong outflow. Many problems were encountered with the vast amount of data, such as verification of strong surface winds, and with identifying a particular feature because of different viewing angles. It was decided that to identify such a feature, a detailed examination of the "true" wind field within a gust front producing thunderstorm must be made. Since Doppler radar can only measure the radial wind component, two or more strategically located Doppler radars are required to estimate the three-dimensional wind field. Previous multiple-Doppler research has centered around storms which either produced a tornado or at least developed a mesocyclone. Since many thunderstorms produce strong outflow without developed mesocyclones, I chose to examine a storm which produced no severe weather other than intense straight-line winds. After reviewing many thunderstorms for which dual-Doppler data is available at NSSL, only one case (3 May 1977) seemed suitable for study.

2.1 Synoptic Conditions

On 3 May 1977, a 500 mb shortwave approached Northwestern Texas from the west. Very moist, potentially unstable, low-level air was

pushed northward from the Gulf of Mexico by strong southerly flow. The morning soundings at Amarillo and Midland, Texas were extremely unstable and displayed vertical wind profiles favorable for severe thunderstorm development. The Oklahoma City sounding was only moderately unstable.

A line of moderate to heavy thunderstorms began to develop in the Texas panhandle during the afternoon and moved toward the east-notheast into western Oklahoma in the early evening. With the exception of localized cases of high winds, the severe activity was limited to western portions of Texas and Kansas. As the line moved into central Oklahoma, the storms weakened slightly but the maximum tops remained above 10 km (approximately 33,000 ft). The line moved into the Oklahoma City-Norman area at approximately 2230 CST. Winds at reporting stations were less than 45 knots but broken windows and roof damage were reported in downtown Oklahoma City at 2245 CST.

2.2 Data Collection

The NSSL dual-Doppler radar system consists of two modified FPS-18 radars with 10 cm wavelength. One radar is located at Norman and the other is positioned 41 km away, near Cimarron Airport*, just west of Oklahoma City. The characteristics of the two radars, as they were used for data collection on 3 May 1977, are shown in Table 1.

NSSL Doppler radars provide mean radial wind speeds calculated from many velocity samples in the volume enclosed by the radar beam. This mean velocity is taken to be the velocity at the center radar pulse volume. To gain confidence that the velocity data was positioned

*Cimarron Airport has recently been renamed Page Airport.

correctly, a dual pulse repetition frequency processing system was used. This system allowed intensity data to be acquired during a long repetition period (460 km range) and velocity data during an interspersed short period (115 km range). Comparisons were made between the reflectivity and velocity samples so that each velocity estimate was positioned accurately in space. This helped avoid the problem of velocity samples from multiple trip echoes being displayed at the same range location. Details concerning data acquisition and signal processing techniques are included in Ray et al. (1975) and Sirmans and Bumgarner (1975).

To minimize the error in computing the dual-Doppler winds, the storm must be located within a very restricted area. Brown et al. (1975) describes the NSSL dual-Doppler system and shows the areas of optimum location. The circles shown in Figure 2 represent the location of points subtending angles between the two radar beams. The 90 degree circle is the location where the "best" dual-Doppler wind computations can be made. The uncertainty in the dual-Doppler wind increases as the angle between the two radar beams depart from 90 degrees. The box in Figure 2 indicates the area chosen for the analysis.

Figure 3 shows the location of the squall-line at 2108 CST. This reflectivity display was taken from the Norman Doppler at an elevation angle of 2.1 degrees. At 2116 CST both the Norman and Cimarron Doppler radars began to sector scan the dual-Doppler area. The Norman Doppler collected data from 226 to 288 degrees azimuth (shown as dashed lines in Figure 3) at increments of approximately 0.4 degrees and at elevation angles increasing at increments of approximately one degree from 1.0 to 23.0 degrees. The Cimarron Doppler collected data by sector scanning

between 151 and 254 degrees azimuth (also shown on figure 3) at increments of approximately 0.8 degrees and at elevation angles increasing at increments of approximately 0.5 degrees from 0.3 to 14.2 degrees, and every 1.0 degree from 14.2 to 21.2 degrees. The data spacing along a radial was 150 m for both Norman and Cimarron. The total time for collection at Norman was from 211613 to 212117 CST and 211611 to 212504 CST for Cimarron.

2.3 Analysis Techniques

The dual-Doppler analysis technique used in this research was basically as used by Brandes (1977). The radial velocity and reflectivity measurements were interpolated to grid points spaced at 1 km intervals on horizontal planes beginning at the surface and spaced every 750 m vertically. Barnes' (1964) objective analysis scheme using an exponential weighting function and a circular spheroid with a radius of influence of 1 km was incorporated. The weight function was defined as:

$$\text{weight function} = \exp(-r^2/4k) \qquad (1)$$

where r was the distance from the grid point to the datum location and k was a parameter determining the shape of the weight factor and was related to the density of the observed data. For this research k was chosen to be equal to 0.09. Figure 4 is an illustration of weight placed on a datum point as a function of distance from the grid point. Any data located outside the radius of influence (r_1) had no effect on the result at the grid point. The weight values varied from 1.0, when the datum location coincided with the grid location, to 0.06 at the radius of influence.

This objective analysis routine resulted in 11 horizontal planes (35 x 35 km), with radial wind components from the two radars plotted at 1 x 1 km grid spacing. The reflectivity values at each grid point were interpolated from Cimarron data only.

During the time interval involved in collecting the data (approximately eight minutes) the storm was assumed in quasi-steady state. All portions of the storm were also assumed to have moved at the same speed in order that the radar observations could be adjusted to a common reference time (2120 CST). This was done by relocating the datum point by the distance obtained from multiplying the storm motion (250 degrees at 8.3 m s^{-1}) by the difference between the sampling time and reference time.

After the radial wind components were obtained at each of the grid points, they were broken down into their components with respect to a Cartesian coordinate system. A radial velocity is related to its Cartesian wind components by the following relationship.

$$V_{Nor} = (x_N u + y_N v + z(w+V_t))/R_N \qquad (2)$$

$$V_{Cim} = (x_C u + y_C v + z(w+V_t))/R_C \qquad (3)$$

V_{Nor} and V_{Cim} are the radial velocities sampled by the Norman and Cimarron Doppler radar, respectively. The x, y, and z are the East, North, and vertical distances from the corresponding radar and the slant range, $R = (x^2+y^2+z^2)^{1/2}$. Likewise, u, v, and w are the wind components to the East, North, and vertical at the locations described by x, y, and z. The terminal fall speed (V_t) of the assumed water droplet was obtained from Roger's (1964) estimate from reflectivity measurements (Z).

$$V_t = 13.8\ Z^{1/14} \tag{4}$$

This estimate of V_t was adjusted slightly by using the Foote and du Toit (1969) density-height correction.

The third equation incorporated was the analastic continuity equation (Ogura and Phillips, 1962).

$$\frac{\partial w}{\partial z} = -\left(\frac{\partial u}{\partial x} + \frac{\partial v}{\partial y}\right) + kw, \tag{5}$$

$k = -\frac{\partial \ln \rho}{\partial z}$ (taken from the standard atmosphere $10^{-4}\ m^{-1}$).

The three equations were solved simultaneously for u, v, and w using a finite-difference technique and five iterations. The lower boundary conditions required w to be equal to zero at the surface.

Problems can arise when attempting to apply the continuity equation to convective activity. The horizontal wind fields were determined with little uncertainty since the sampled Doppler radial velocities were nearly horizontal. However, the poor sampling of the winds in lowest levels by the Doppler radar can lead to a poor estimation of the divergence and subsequent vertical motion near the ground (Ray and Wagner, 1976). This initial bias in the vertical motion can add to errors which tend to accumulate in the numerical integration of the continuity equation over several levels.

2.4 Interpretation of Data

Eleven horizontal cross sections of the dual-Doppler data set were analyzed, beginning at the surface and increasing vertically every 750 m up to 7.5 km. General kinematic features of the cross sections at heights of .75, 2.25, 3.75, and 5.25 km are described in the text and illustrated in Figures 5 through 8. The horizontal projections of wind velocities are relative to the moving squall-line (250°/8.3 m s^{-1} has been subtracted from each velocity vector). The velocity vectors are represented by arrows, with the length of the arrow proportional to wind speed. Overlayed on the flow patterns are the corresponding reflectivity contours. Alongside the flow patterns are contoured displays of vertical velocity and horizontal divergence. The X and Y distances are the distances to the east and north of Norman, respectively.

2.4.1 Dual-Doppler Wind Fields

Perhaps the most distinctive feature at the height of 0.75 km (figure 5) was the horizontal divergence along a line corresponding to where the X-distance was equal to -40 km. This divergence pattern was typical of a downdraft entering the boundary layer near the earth's surface, where the vertical motion was forced horizontal (Fankhauser, 1976). The general area of divergence corresponded well with an area of high reflectivity. This gave support to the theory of a precipitation-drag enhanced downdraft. Vertical velocity contours also showed a general area of descending motion (approximately -3 m s^{-1}) in the areas of highest reflectivity. The storm in the lower right-hand portion (southeast) of the area was the most intense cell. Strong low level inflow

into this cell resulted in an area of high convergence (9.3×10^{-3} s^{-1}) and subsequent updraft (6 m s^{-1}). A region of cyclonic shear is also located coincident with the updraft (maximum vorticity, 9.4×10^{-3} s^{-1}).

A large area of divergent flow could still be seen at 1.5 km (not shown) but the magnitude of divergence had significantly decreased. At 2.25 km (figure 6) the divergent flow had decreased to a point where values in excess of 2.5×10^{-3} s^{-1} were confined to a small area along the back side (west) of the squall-line. A weak convergence area was beginning to appear in the areas of high reflectivity. This was above an area of strongly divergent flow at 0.75 km. In fact, the maximum value of convergence along the back side of the squall line (5.3×10^{-3} s^{-1}) was located at a position just 1 km to the southwest of a 45 dBZ reflectivity core. This was also the location of divergence greater than 5×10^{-3} s^{-1} at a height of 0.75 km. This convergent flow appeared to be feeding the downdraft as the strength of the downdraft had increased to -10 m s^{-1}.

The convergence area along the back side of the squall-line was very pronounced at 3.75 km (figure 7). The wind flow relative to the storm at 2.25 km was generally from the east to southeast and appeared to flow through the squall-line. At 3.75 km, the winds along the leading edge were still quite strong and from the east-southeast, but along the back side, the flow had shifted to the west. This led to a broad area of convergence coincident with the large area of maximum reflectivity (>35 dBZ).

Three different phenomena appeared to act together to intensify the downdraft. The area of highest reflectivity indicates abundant precipitation and precipitation drag may be acting to direct the air downward.

Secondly, the dry mid-level air, as indicated by the Oklahoma City sounding, flows into the back side of the storm, evaporates cloud droplets, cools, becoming less bouyant, and descends into the downdraft. Finally, the convergent flow was dynamically forced air downward.

At 5.25 km (figure 8) the strong east-southeasterly flow into the front side of the storm had weakened considerably. The wind was still westerly into the back side of the squall-line, but the overall result was a significant decrease in the area of strong convergent flow. The downdraft had a maximum speed just over 15 m s^{-1} at 5.25 km. Analyses were also completed at heights of 6.0, 6.75, and 7.5 km but are not shown. The horizontal flow patterns above 5.25 km were even smoother, with the only significant divergence being associated with the intense cell in the lower right corner of the area.

These horizontal profiles seemed to support the idea of mid-level air being the source of the downdraft and subsequent outflow. First the low level (<1 km) flow was highly divergent, indicative of a downdraft being forced horizontal at the earth's surface. Secondly, the outflow (easterly winds) along the back side of the squall-line switched to inflow (westerly winds) at the mid-levels (3 - 5 km) resulting in strong convergence directly above the divergent flow near the ground. Finally, the horizontal flow in the upper levels (>6 km) showed basically a southerly component to the wind with very little divergence noted.

2.4.2 Θ_w Analysis

To help demonstrate that the outflow air did originate at the mid-levels of the storm, a wet bulb potential temperature (Θ_w) analysis

of the 4 May 1977, 00Z Oklahoma City sounding (figure 9) was performed. In the downdraft, the air from the mid-levels is cooled through evaporative cooling and descends as moist adiabatic. By comparing the Θ_w of the outflow air at the surface, with the Θ_w values computed from the Oklahoma City sounding, an indication of the levels where the air originated was obtained. At 2120 CST (time of the dual-Doppler analysis) the low-level divergent flow was very near the NSSL mesonetwork site at Tuttle, Oklahoma, approximately 33 km west-northwest of Norman. The temperature at Tuttle had decreased from 78°F (25.6°C), in advance of the gust front, to 61.4°F (16.3°C) at 2122 CST, when the downdraft was nearly overhead. The wind at 2122 CST was from 205° at 30 to 36 kts. At 2126 CST the wind shifted to the southeast (135 to 155°) at 20 to 30 kts, indicating the core of the downdraft had just passed overhead. The surface pressure at 2126 CST was 965 mb and the relative humidity was 100 percent. This converts to a surface Θ_w of 17.2°C. The lowest temperature recorded at any of the mesonetwork sites was 58.9°F (14.9°C) at Blanchard, Oklahoma, 23 km southwest of Norman. This converts to a Θ_w equal to 16.3°C, narrowing the height interval very little.

Since Θ_w is a conserved property, the outflow air appears to have originated at a level between 2.0 and 6.0 km AGL (see figure 9). If this was the case, it would agree well with the dual-Doppler analysis, in that the convergence boundary begins to appear just above 2 km, increases in intensity up to approximately 4 km, then decreases again becoming nearly zero above 6 km. One may conclude, on the basis of such evidence that strong downdrafts and subsequent intense low-level outflow result from intrusion of mid-level air into the squall-line.

2.4.3 Identification of Downdraft

As shown by the dual-Doppler and Θ_w analyses, the convergent boundary at the mid-levels of the storm (3 to 6 km) was the main source of the downdraft and subsequent divergent outflow near the surface. In real-time operations, other factors would need to be considered in order to identify a convergent boundary aloft as the source of a downdraft as opposed to an updraft. A few ideas to help make this distinction are explained below.

1. The strongest convergence associated with an updraft is generally located on the low-levels of the storm (see figure 1). This is the source of the warm moist air, which is essential to sustain a strong updraft. The updraft region of a storm then generally reaches an area of non-divergence in the mid-levels before it becomes highly divergent near the top. However, if the convergent flow at the mid-levels is associated with the updraft, reflectivity values would either remain nearly constant or possibly increase as the storm is sampled at higher levels. A weak echo region (Lemon, 1978) may also appear in the reflectivity display. Finally, as the top of the storm is sampled, a strong divergent flow would be expected above the updraft core.

2. The strongest convergence associated with a downdraft appears to be located at the mid-levels of the storm. As opposed to an updraft, the reflectivity values would appear to decrease as the storm is sampled above the convergent portion of the downdraft. If the low-levels of the storm could be seen, a divergent flow would be expected almost directly below the convergence in the mid-levels.

3. The source of the air forced into this mid-level convergent boundary may also give an indication of whether it is feeding an updraft or downdraft (figure 1). If the convergent flow is primarily a result of midtropospheric air being entrained into the backside of the storm, one would expect this type of air to be the source of a downdraft. The opposite would also be true; if the convergent flow is primarily a result of the inflow air along the leading edge of the thunderstorm, the air would generally be moist and unstable, indicative of an updraft.

3. RECONSTRUCTION OF SINGLE-DOPPLER WINDS

As previously stated, this research was aimed at real-time detection of those thunderstorms likely to produce strong surface winds by using a single-Doppler radar. The dual-Doppler analysis was performed only to obtain the three-dimensional wind field within a squall-line known to have produced high winds. If the dual-Doppler wind field constructed is typical of other high wind cases, this wind field can be used as a model for detection of future storms.

3.1 Conversion Technique

The question that arises is how this three-dimensional wind field would appear when viewed by only a single-Doppler radar. This was accomplished by using basic geometric relationships illustrated in Figure 10. The grid points and the u, v, w, and V_t wind vectors are those computed in the dual-Doppler analysis. The radial distance (R) to the grid point was computed using

$$R = (\Delta x^2 + \Delta y^2 + \Delta z^2)^{1/2}. \qquad (6)$$

The distance east of the radar is given by Δx, north by Δy, and vertical by Δz. The radial component of each of the Cartesian wind components was computed as follows:

$$u_r = u\,(\Delta x / R), \qquad (7)$$

$$v_r = v\,(\Delta y / R), \qquad (8)$$

$$w_r = (w + V_t)(\Delta z / R). \quad (9)$$

Summing these components yielded the final radial wind velocity (V_r) at the grid point,

$$V_r = u_r + v_r + w_r \quad (10)$$

The angle from which the storm is viewed can be changed by altering the values of Δx and Δy which is equivalent to shifting the location of a fictious radar relative to the storm. For this study, it was decided to locate the radar at a distance equal to 150 km and rotate the location of the radar, calculating the radial wind field at 30° intervals. By viewing the storm at a significant distance, the plane being sampled by the radar is nearly horizontal, thereby eliminating the problem of accounting for vertical velocities within the storm. Also, at this distance, low-level (< 1 km) outflow winds could not be seen by the radar.

The conclusion reached by the dual-Doppler analysis was that the horizontal convergence signature at mid-levels of the storm may indicate a strong downdraft and intense outflow. Maximum convergence was seen at a height of 3.75 km. Therefore, this was the level at which the radial wind field and divergence were computed. Since grid points set up for the dual-Doppler analysis were in a Cartesian coordinate system, horizontal divergence was computed using the Cartesian coordinate system and the u and v components of the radial wind vectors. This horizontal divergence is an accurate estimate of radial divergence as long as the radar elevation angle remains small.

Viewing angles, in the following discussion, were computed by subtracting the angle from which the storm is moving from the azimuth

at which the radar is oriented. For example, if the storm moves from 250° and the radar azimuth is 280° when viewing the storm, then the viewing angle is 30°. If the azimuth of the radar was 100°, instead of 280°, then the viewing angle would be -150°. When viewing a storm volume from a considerable distance, the radial velocities from a central viewing angle of 30° and -150° will be equal but of opposite signs. On either side of the central viewing angle, the values are only approximately equal. The divergence values will also be nearly equal. Therefore, instead of illustrating the radial wind fields from every 30° around the entire storm, only those between 0° and 150° are shown, with the opposite angle ($\pm 180^{\circ}$) shown in parenthesis.

The results of the dual-Doppler analysis and the program written to convert the dual-Doppler wind velocities back to radial velocities were tested by using a Δx and Δy equal to the distances from the Norman Doppler radar to the storm. The resulting radial velocities were exactly (within less than 0.1 m s^{-1}) the same as the original data set inserted into the dual-Doppler analysis after interpolating to the grid points. The same check was performed by switching the fictious radar to the location of the Cimarron Doppler radar and again the original wind field was returned.

3.2 Results

The radial wind field that would be seen if the storm were moving directly toward or directly away from the radar is shown in Figure 11. As would be expected, convergence values exceeding 5×10^{-3} s^{-1} are seen in the same vicinity of the storm as the dual-Doppler analysis. Because the full strength of the east-southeasterly flow cannot be observed from

this viewing angle, the large area of convergence exceeding 2.5 x 10^{-3} s^{-1} is considerably smaller.

Moving clockwise around the storm changing the viewing angle to 30° (-150°), the radial wind field would appear as that shown in Figure 12. The areas of convergence exceeding 5 x 10^{-3} s^{-1} are again basically the same, but the area of convergence exceeding 2.5 x 10^{-3} s^{-1} is significantly larger than when viewed from a location where the storm was directly approaching. This result was obtained since nearly all of the strong east-southeasterly flow into the front of the storm can be seen without eliminating the effect of the westerly winds entrained into the rear of the storm. From this angle it is apparent that a strong convergence boundary exists and there would be a pssibility of high surface winds.

Viewing the storm from 60° (-120°) off of storm motion (figure 13), showed the convergence boundary decreasing significantly. Only one small area of convergence exceeding 5 x 10^{-3} s^{-1} is now evident. The area of convergence exceeding 2.5 x 10^{-3} s^{-1} is, however, still substantial and may be large enough to give an indication of a significant downdraft. The strength of the east-southeasterly wind is very noticeable, but the westerly flow into the backside of the storm is not obviously reflecting its true strength.

As was expected, the convergence boundary is much more difficult to see when viewed from an angle perpendicular (±90) to the storm motion (figure 14). There are, however, values of convergence as high as 3.9 x 10^{-3} s^{-1} along the backside of the storm (located at -64, 134). This result was initially surprising, but on further study it can be seen that the convergence boundary is a result of the east-southeasterly flow

meeting the westerly flow. Viewing the storm from the south-southeast would yield a higher convergence value due to the radial components of the east-southeasterly wind.

One might expect the convergence boundary to appear stronger again as the viewing angle increases from 90° toward 180°. However, as one can see from Figure 15, this is not true. When viewing the storm from 120° (-60°), the convergence boundary is nearly nonexistent. The radar is viewing the storm from an angle which is nearly perpendicular to both the east-southeasterly flow and the westerly winds. It is felt that identifying a downdraft by a convergent signature from this angle would be nearly impossible.

Figure 16, illustrating the last viewing angle (150° or -30°), shows a very broad area of noticably weak convergence. The viewing angle is still approximately 70° off the westerly flow into the backside of the storm and the magnitude of the radial component from the east-southeasterly flow decreases very slowly as it penetrates the storm front. This resulted in a wide area of weak converging flow with only a very small area of convergence equalling $3.5 \times 10^{-3}\ s^{-1}$.

As was expected, the angle from which the storm is viewed is very important. If the storm is directly approaching the radar, or if the viewing angle is less than 40°, it appears that a very accurate estimate of the true convergence can be made. As the viewing angle increases, the magnitude of convergence decreases until the convergent boundary becomes nearly indiscernable at a viewing angle greater than 110°. At approximately 140° the convergence values have increased again to a point where a convergent boundary could be identified. The convergence values continue to increase as the viewing angle approaches 180°.

4. APPLICATIONS OF RESULTS

To this point, nearly all of what is contained in this research was based strictly on the analysis of one storm and the assumption that this storm had the same basic features as most storms that produce strong low-level outflow. To help justify this assumption, single-Doppler data collected from three different gust front cases that occurred during the spring of 1978 are discussed. None of the three cases contained a mesocyclone but all resulted in damaging surface winds.

4.1 Multimoment Display

To obtain a more detailed velocity profile during real-time operations, the NSSL multimoment display (Burgess et al., 1976) was used. The multimoment display is a field of arrows where arrow length is proportional to intensity (reflectivity), arrow deflection to mean velocity, and arrowhead size to spectral width (see figure 17). Arrows pointing right indicate zero radial velocity, arrows pointing toward the top or bottom of the display are plus or minus one-half the unambiguous velocity respectively (normally ± 17 m s^{-1}), with positive velocities defined as away from the radar. The unambiguous velocity varies according to the pulse repetition frequency (PRF) as shown in Table 1. Arrows pointing toward the left are equal to plus or minus the unambiguous velocity (normally ± 34 m s^{-1}). These arrows must not be confused with

the arrows shown in previous figures where arrow length indicated magnitude of the velocity. The displayed velocities are radial components of motion only and should not be interpreted as true velocity vectors of the horizontal air flow as was the case in the dual-Doppler analysis.

4.2 21 June 1978

On 21 June 1978 a strong squall-line developed during the late morning in north central Oklahoma and moved rapidly southeastward toward the Oklahoma City area. Extensive wind damage was reported and wind gusts of over 60 kts were recorded at both Oklahoma City and Norman shortly after noon. A reflectivity display of the squall-line taken from the Norman WSR-57 is shown in Figure 18.

The squall-line was moving directly toward Norman as the velocity data was recorded. The box in Figure 18 was the section of the storm on the multimoment displays shown in Figures 19 and 20. A storm motion of 320^{o} at 10 m s^{-1} was subtracted from the data. The distance between data points was approximately 1.0 km.

At 1201 CST the Doppler radar was scanning at the lowest elevation angle (0.2^{o}) intersecting the storm at an average height of 400 m (figure 19). An interesting point was the similarity of this storm with the 3 May 1977 squall-line. Notice the divergent flow along the area marked with the letter "D" where the downdraft was apparently forced into horizontal flow near the earth's surface. The gust front also seems to appear in the lower right portion of the figure (marked with a dashed line). There was very strong outflow just behind the gust front in the area circled. After adding back in the storm motion, to find the wind speed relative to the ground, velocities exceeded 35 m s^{-1}.

The divergent area at 400 m changed quickly to convergence above a height of 2 km. The most pronounced convergence appeared at a height of 5.1 km (figure 20). The broad area of convergent flow, located at an approximate distance of 66 km, was almost directly above the divergent flow at 400 m. Maximum convergence (approximately equal to 1.6×10^{-2} s^{-1}) was in the area located at 300^{o} at 60 km; this was directly above the maximum winds at 400 m. Convergence values were of nearly equal magnitude at 4 km (not shown) but decreased as the storm was sampled both above 5.1 km and below 4 km.

4.3 31 May 1978

On 31 May 1978 numerous severe thunderstorms were reported in Kansas, including tornadic storms in the northeastern part of the state. A very strong cell developed just north of the Oklahoma border near the town of Anthony, Kansas during late afternoon, and drifted slowly toward the southeast. Although there were no reports of damage available, two thunderstorm intercept teams from the University of Oklahoma reported a very strong gust front associated with the storm. A photograph of the gust front is shown in Figure 21.

A reflectivity display from the Norman WSR-57 (figure 22) shows the location of the storm was approximately 200 km north-northwest of Norman. At the lowest elevation angle (0.2^{o}), the Doppler radar was sampling the storm at a height of 3.2 km. The winds below a height of 1 km obviously could not be seen, and therefore, a warning based strictly on observed outflow could not be issued. The convergence was very strong at a height of 3.2 km with the maximum convergence (approximately equal to 1.9×10^{-2} s^{-1}) located in the area outlined in Figure 23. The magnitude

of convergence at 4.6 km (figure 24) was only slightly less, but values decreased rapidly as the storm was sampled at even higher levels.

4.4 4 April 1978

On the evening of 4 April 1978 a strong thunderstorm developed in southwest Oklahoma and moved very rapidly toward the north-northwest. JDOP was not in operation on 4 April due to the forecast of no severe weather. A computer technician was working late that evening testing modifications to the Doppler software. He began to collect data at approximately 2200 CST. Sonce JDOP was not in operation, the Doppler data was not recorded, however the multimoment data was recorded and was therefore available for post analysis.

This storm may have gone completely unnoticed had it not produced a gust of 60 kts at the NSSL mesonetwork site at Seiling, Oklahoma. Just over 20 minutes before the strong wind, the multimoment data shown in Figures 25 and 26 were collected. The pulse repetition frequency (PRF) during collection was 930 Hz, thereby lowering the unambiguous velocity interval to ± 24.3 m s^{-1} as opposed to ± 34.2 m s^{-1} under the normal (1300 Hz) PRF. The arrows pointing toward the bottom of the display therefore represent -12 m s^{-1} as opposed to -17 m s^{-1}. The storm was located at 280^{o} at 140 km from the radar and was moving from approximately 200^{o} at 15 m s^{-1}.

As would be expected, the convergence appeared much weaker than the previous storms discussed, since the viewing angle was approximately 80^{o} off storm motion. At the height of 3.2 km (figure 25), the maximum convergence was approximately equal to 4×10^{-3} s^{-1}. The magnitude of the convergence increases very little at 4.5 km (figure 26), where the

maximum convergence was equal to approximately 5×10^{-3} s^{-1}. As in the other storms, the convergence values again decreased as the storm was sampled at higher levels.

These three cases were chosen to illustrate the mid-level convergence from three distinctively different storms. The 21 June case was a rapidly moving squall-line, very close to the Doppler radar. At low elevation angles, the strong outflow could easily be seen, actually eliminating the need to scan higher in the storm. The 31 May case was a slow moving storm located 200 km from the radar, where seeing the low-level outflow would be impossible. Thus, one would be forced to look at the mid-levels for an indication of possible strong low-level winds. The 4 April case was a rapidly moving storm, located 140 km from the radar and moving nearly perpendicular to the radar beam. From this distance the low-level outflow could not be seen and from this angle the convergence boundary also appeared weak. Although all three cases were considerably different, a convergence boundary was present in all cases and strong surface winds were reported from each storm.

5. SUMMARY AND CONCLUSIONS

The dual-Doppler analysis of 3 May 1977 squall-line yielded valuable information to further understanding of the three-dimensional wind field within a gust-front-producing thunderstorm. The low-level outflow was highly divergent, indicative of a downdraft being forced into horizontal flow by the earth's surface layer. The outflow near the surface undercut inflow along the leading edge of the storm at a height just above 1 km, resulting in weakening the divergent flow until it became nearly nonexistent above 2 km. Outflow along the backside of the storm shifted slowly to dry air inflow just above a height of 3 km, yielding a strong convergent boundary directly above the divergent flow near the surface. The convergent area increased in size and strength up to 3.75 km, then slowly deteriorated until it was hardly noticeable above 6 km. This leads to the conclusion that the mid-level (3 to 6 km) air was the main source of the downdraft air responsible for the strong surface outflow. A Θ_w analysis helped verify this conclusion.

If this convergence boundary is typical of most thunderstorms producing strong low-level outflow, then the observance of this phenomenon in real-time may aid in forecasting such an event. However, since real-time operations necessitate using a single-Doppler radar, the dual-Doppler wind field was converted back to radial wind fields that would be viewed from various angles by a single-Doppler radar. The horizontal cross section

at a height of 3.75 km was used in the conversion since this was the level of maximum convergence in this storm. The convergence boundary was easily identifiable when the storm was moving directly toward the radar. The most difficult angle from which to identify the convergence was from the right rear and left front quadrants of the storm.

To further illustrate the possible use of the convergence signature in real-time operations, single-Doppler data analyzed on three thunderstorms known to have produced strong surface winds were examined. In all three cases, a strong convergent boundary was present in the mid-levels of the storm. The convergence values then decreased with height as the radar scanned above or below the mid-levels.

The conclusions reached in this research were based on a preconceived model of a thunderstorm (as described in section 2.4.3). Therefore, if a thunderstorm does not fit this general model, problems may be encountered in applying these results. An example of this type of thunderstorm would be a right-moving storm (moving to the right of the mid-level winds). In the thunderstorm cases discussed in this research, the convergent boundary was oriented nearly perpendicular to storm motion; this may not be the case in a right-moving storm. Caution must therefore be exercised before applying these results in real-time operations.

During the spring of 1979, JDOP will continue to test the feasibility of the Doppler radar in real-time operations. Using the results from the analysis of the 3 May 1977 case, along with the single-Doppler data obtained from the gust front cases in 1978, a graph showing the various viewing angles versus the strength of the convergence seen from that angle was compiled (figure 27). If JDOP forecasters were to use

this graph in real-time operations, many factors must also be taken into account. Some of these are explained below.

1. The values shown in the graph are estimates of the minimum values of convergence felt necessary to produce a downdraft strong enough to result in damaging winds ($\geq$ 50 kts) at the surface. Although these minimum values may be exceeded at a particular point, it also appears that a general area of convergence, as was present in all the storms studied, would be required to sustain a strong downdraft.

2. Although the actual level of the strongest convergence varied somewhat in the thunderstorms studied, the convergence boundary was present over a depth of at least 2 km in all 4 cases. As illustrated by the continuity equation, the depth of the convergent flow is as important as the magnitude of the convergence at any particular level.

3. Another factor which should be considered is the atmospheric conditions during the day. In particular, the flow at 600 to 500 mb seems very important. The dry air inflow along the backside of a storm would appear to be oriented in the same direction as the 600 to 500 mb winds. If an estimation of these winds was known in advance of radar operations, an estimate of the strength of inflow into the rear of a storm can be made by using the radial component of velocity and the orientation of the radar beam relative to this inflow. A storm similar to the 4 April case, where the convergence boundary appeared weak, may then be detected as a thunderstorm likely to produce strong surface winds. Therefore, the values in Figure 27 are only a guideline, and many storms will have to be sampled before any statistical evidence can be compiled to provide a similar representation for use outside a research environment.

There are many problems which need to be solved before the ultimate task of forecasting strong low-level outflow is conquered. One very significant problem which became apparent during this research is to resolve a way to forecast winds from thunderstorms moving at an angle of 110° to 150° (or -30° to -70°) relative to the radar. This appears to be a blind spot for seeing the convergence boundary even when it is known to be present. If there are convergence values which are indicative of outflow exceeding 50 kts, then is there a direct correlation between the magnitude of convergence and strength of the outflow winds which would aid in forecasting the peak wind? To obtain a lead time on high wind advisories, research also needs to be accomplished on the time difference between the development of the convergence boundary and the observance of high winds at the surface. For an effective advisory, an expected duration time for the forecast winds need to be computed. These are only a few of the more obvious problems. Many more exist and many more need to be answered before the problem of forecasting thunderstorm induced high winds is solved.

All thunderstorms have differing features or characteristics. It is also apparent that there are some characteristics which appear only in thunderstorms which produce a particular phenomenon. This research indicates mid-level convergence may be a characteristic that appears in thunderstorms which produce a strong downdraf. and subsequently strong outflow. By identifying a feature in the mid-levels of the storm, the problems of warning on storms located at a distance in excess of 100 km or storms with a gust front out ahead of the precipitation would be eliminated. The author believes that experienced forecasters with a thorough

understanding of thunderstorm dynamics can use this convergence boundary as a forecasting tool when using a single-Doppler radar to warn on thunderstorm induced high winds.

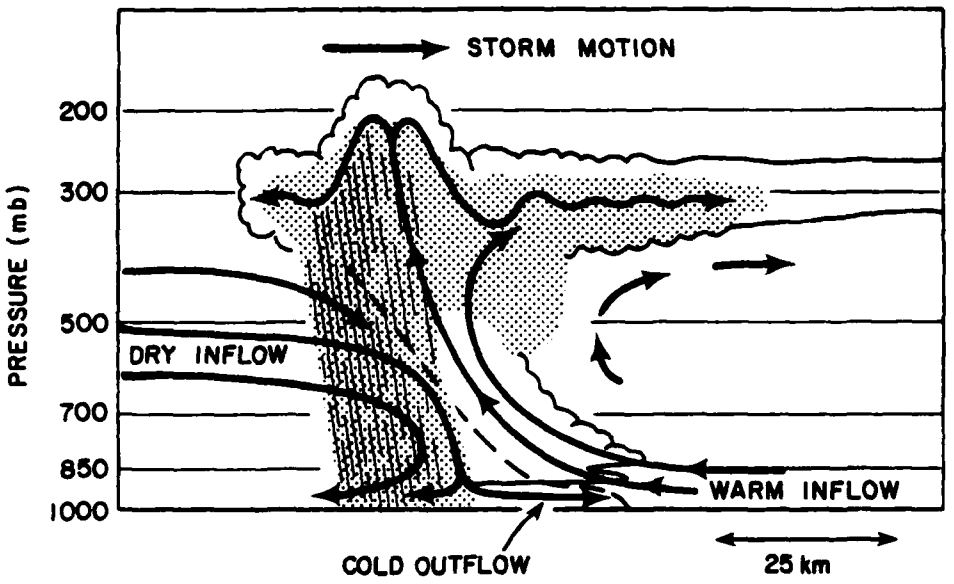

Figure 1. Circulation in a typical mature squall-line. Visual cloud boundary is outlined. Precipitation is stippled. Striations denote heavier precipitation. Vertical scale has been exaggerated fivefold compared to the horizontal scale, which is shown at lower right. (Davies-Jones, 1979)

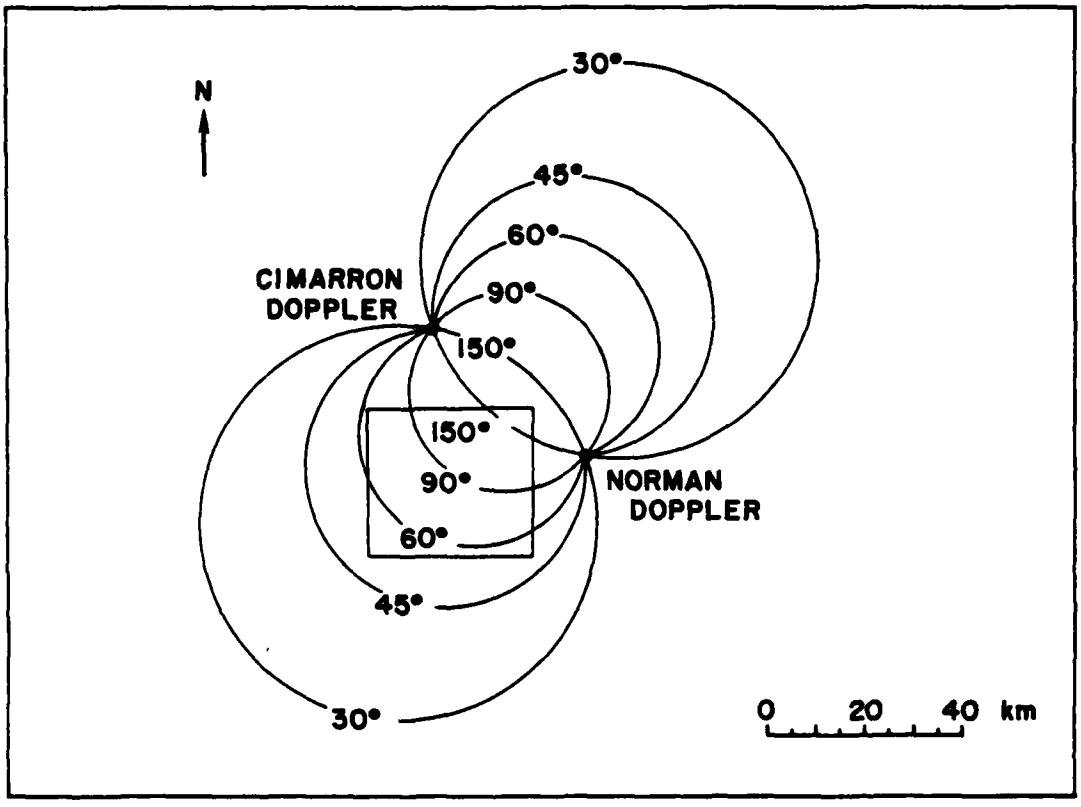

Figure 2. Optimum dual-Doppler radar area. Circles represent the location of points subtending angles between the two radar beams. The square was the area selected for the dual-Doppler analysis of the 3 May 1977 squall-line.

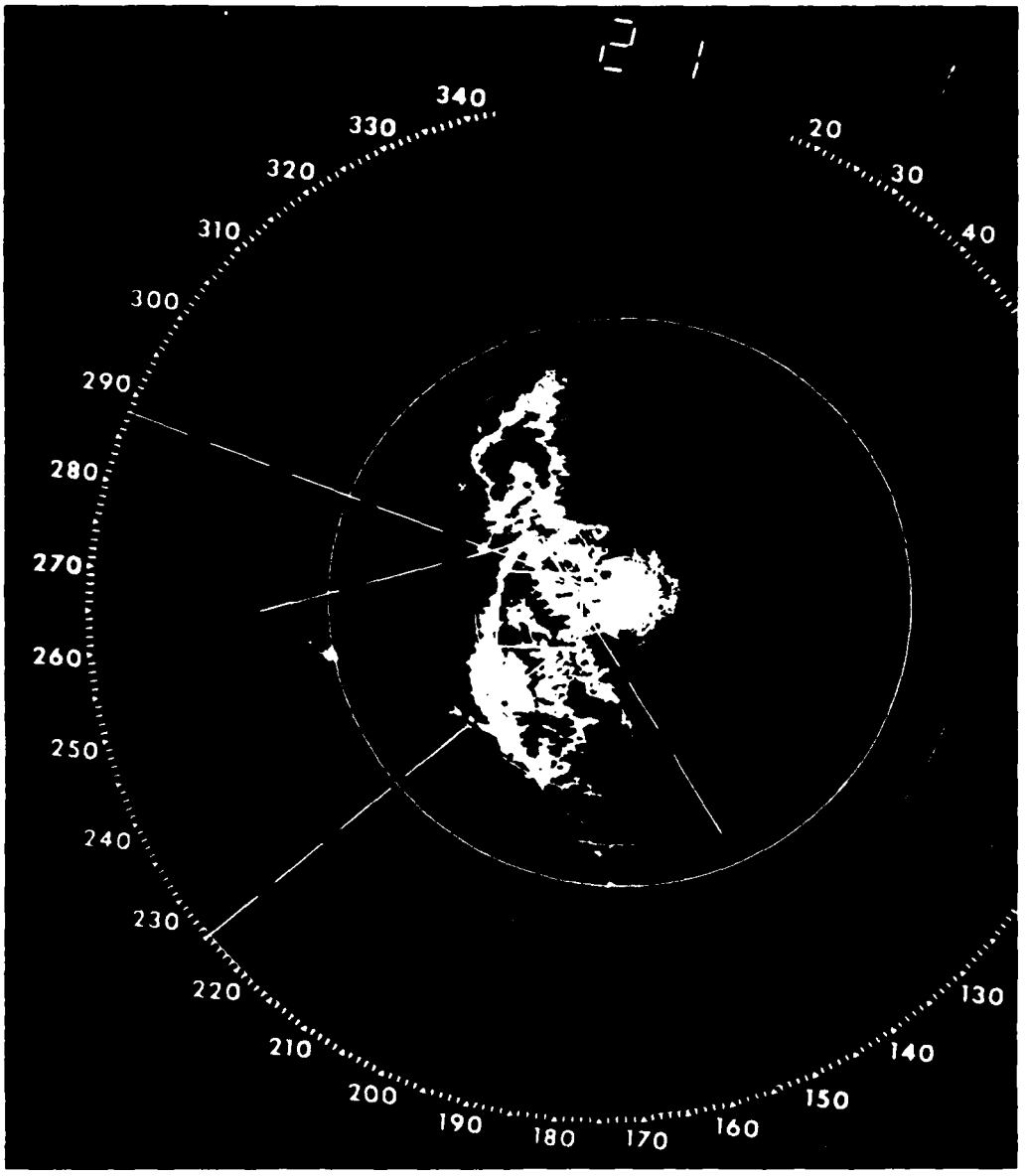

Figure 3. Reflectivity display of the 3 May 1977 squall-line at 2108 CST, taken from the Norman Doppler radar at an elevation angle of 2.1°. The dashed lines represent the areas sector-scanned by the Norman and Cimarron Doppler radars. The square is the area used in the dual-Doppler analysis. Range circles are at 20 km intervals.

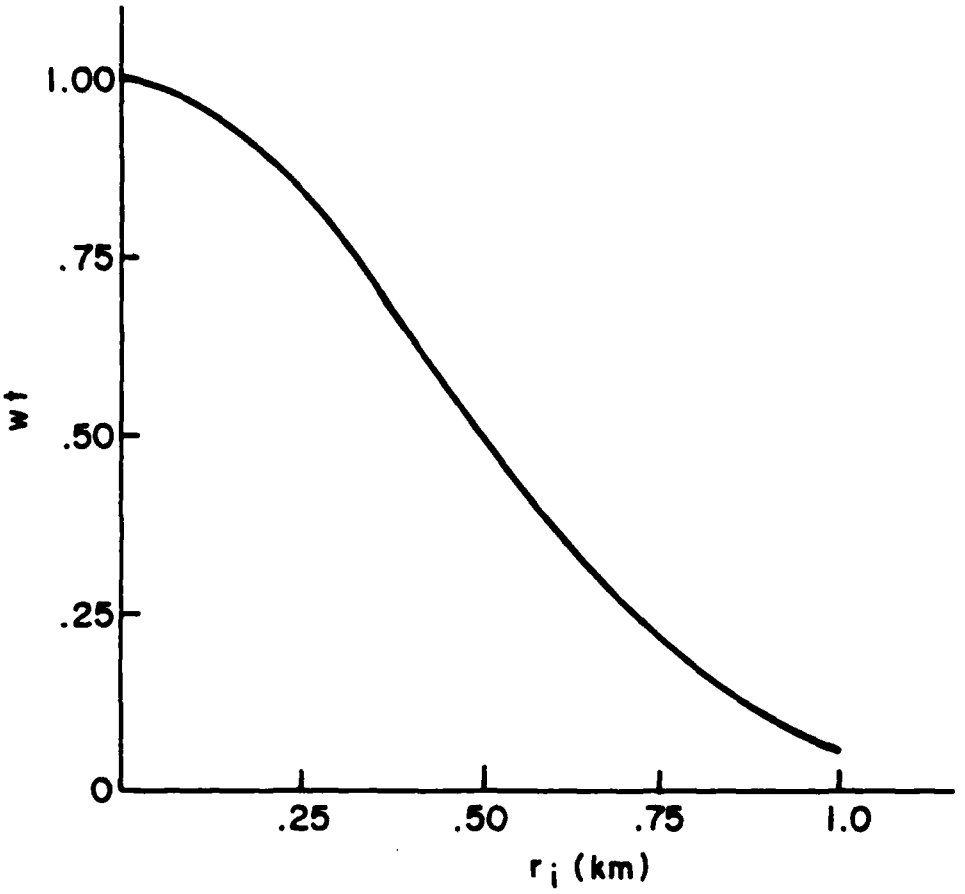

Figure 4. Graph of the weight function versus the distance between the datum point and the grid location used in the interpolation scheme (Barnes, 1964) for the dual-Doppler analysis.

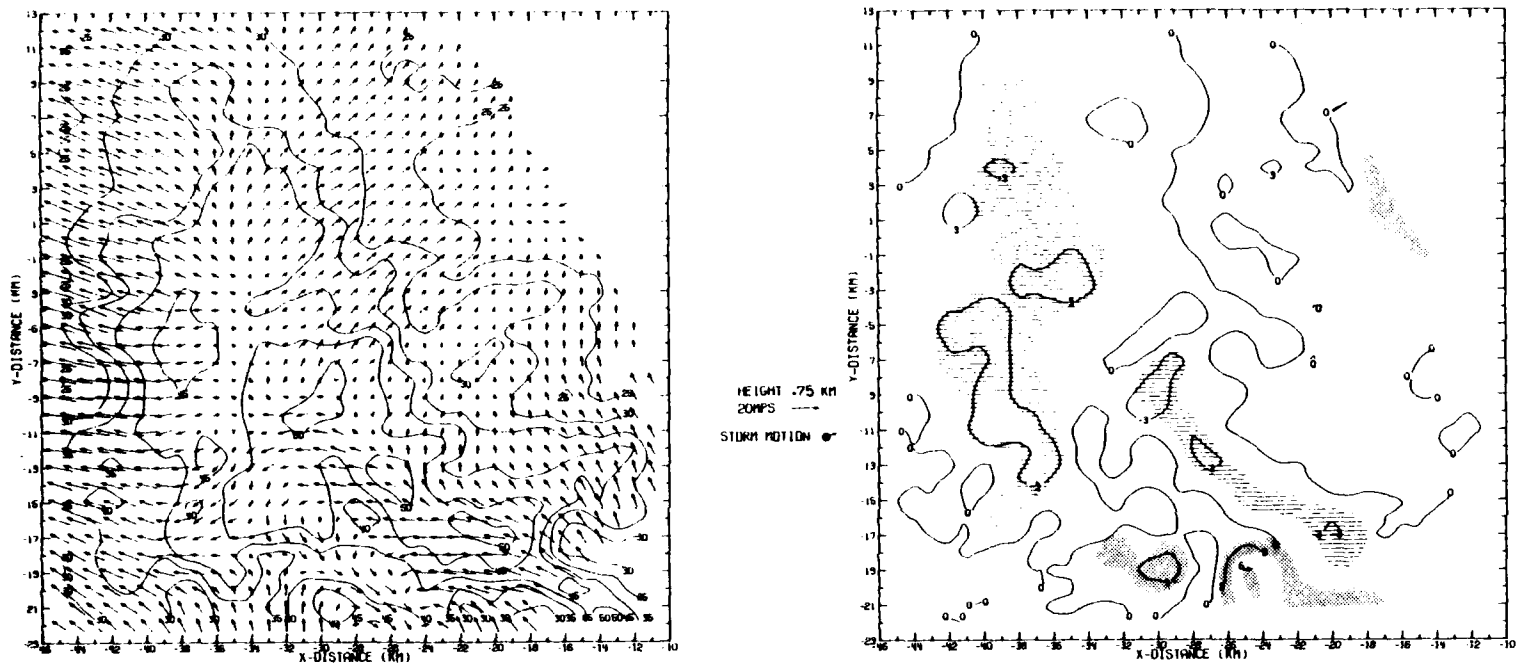

Figure 5. Dual-Doppler wind field analyzed at a height of 0.75 km. On the left is a projection of the horizontal velocity vectors with the arrow length proportional to the speed. A storm motion of 250^{o} at 8.3 m s^{-1} was subtracted from the data. Reflectivity contours at intervals of 5 dBZ are superimposed on the wind field. On the right are contours of vertical velocity in m s^{-1}. The cross-hatched areas are positive values of divergence with negative values (or convergence) shown as stippled areas. The initial cross-hatched and stippled areas are absolute values greater than 2.5×10^{-3} s^{-1}. Open area within the shaded area are values greater than 5×10^{-3} s^{-1}, with the next enclosed shaded area greater than 7.5×10^{-3} s^{-1}.

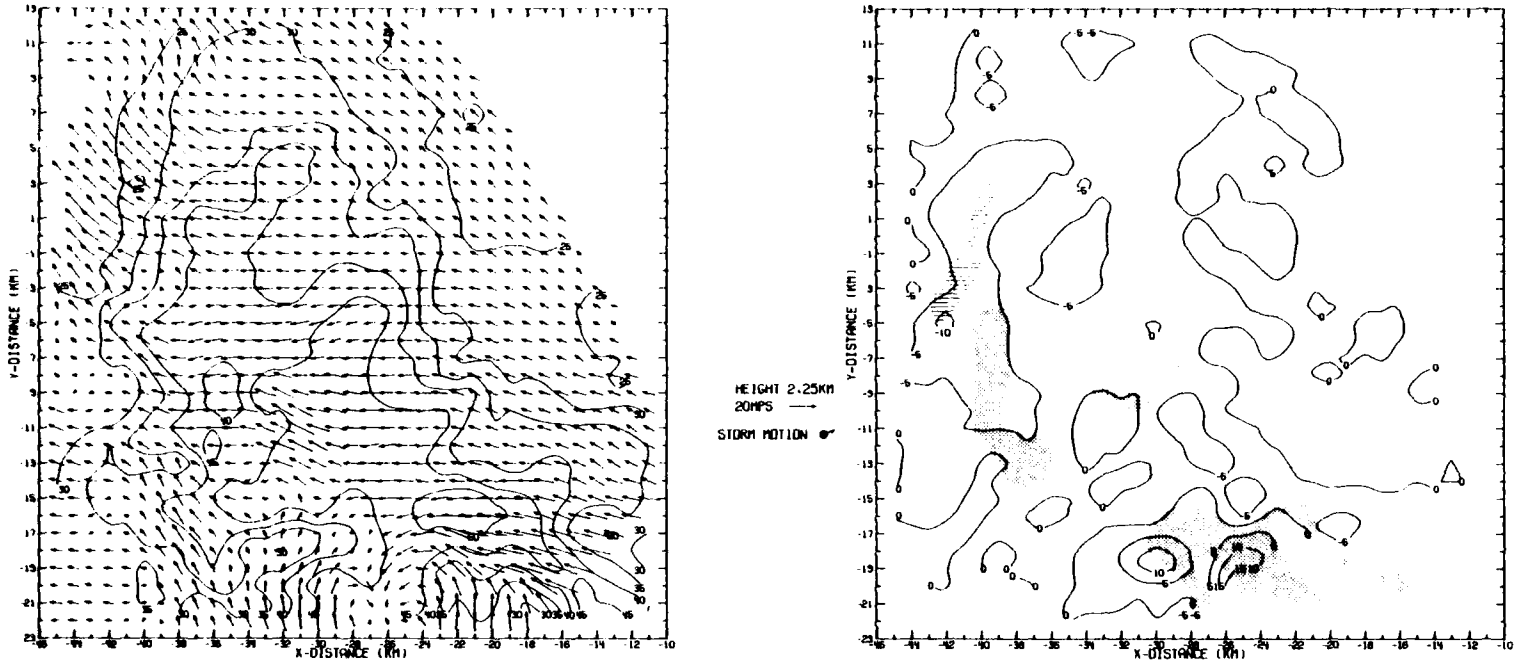

Figure 6. Same as Figure 5 except at a height of 2.25 km.

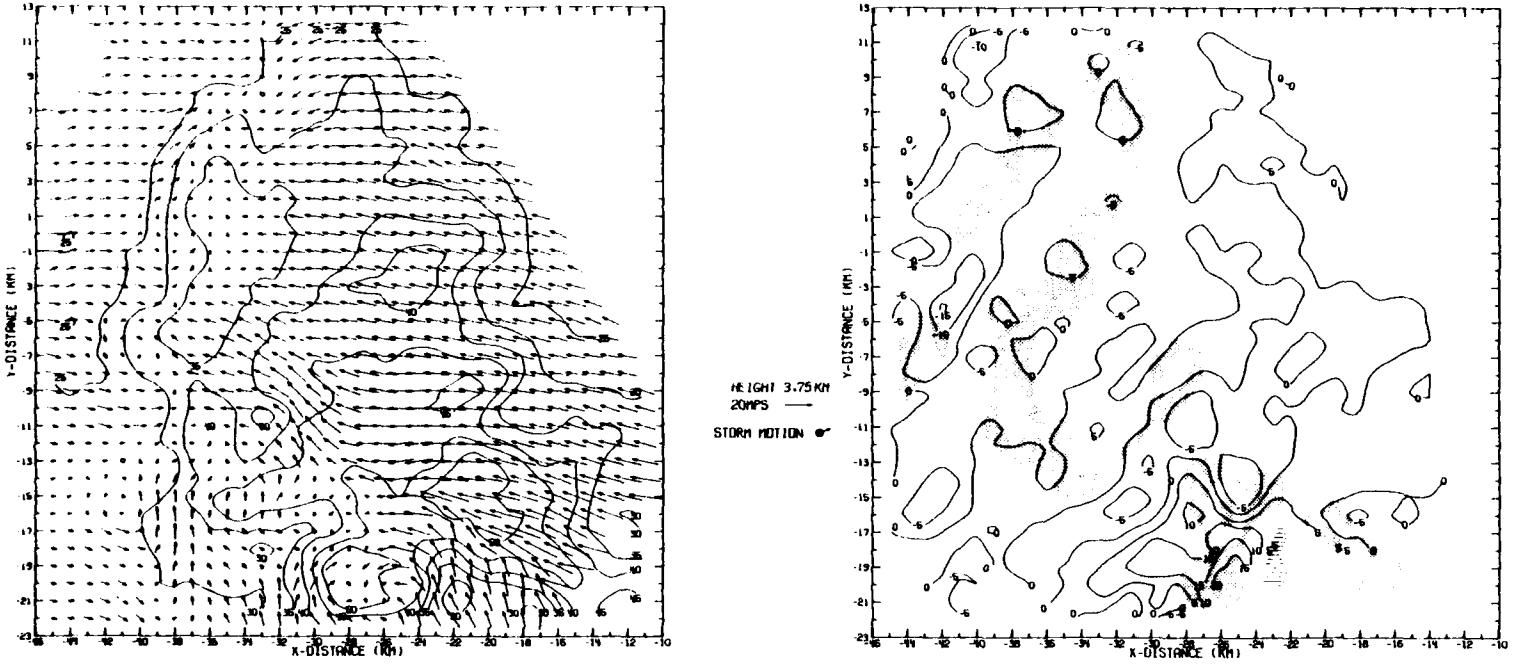

Figure 7. Same as Figure 5 except at a height of 3.75 km.

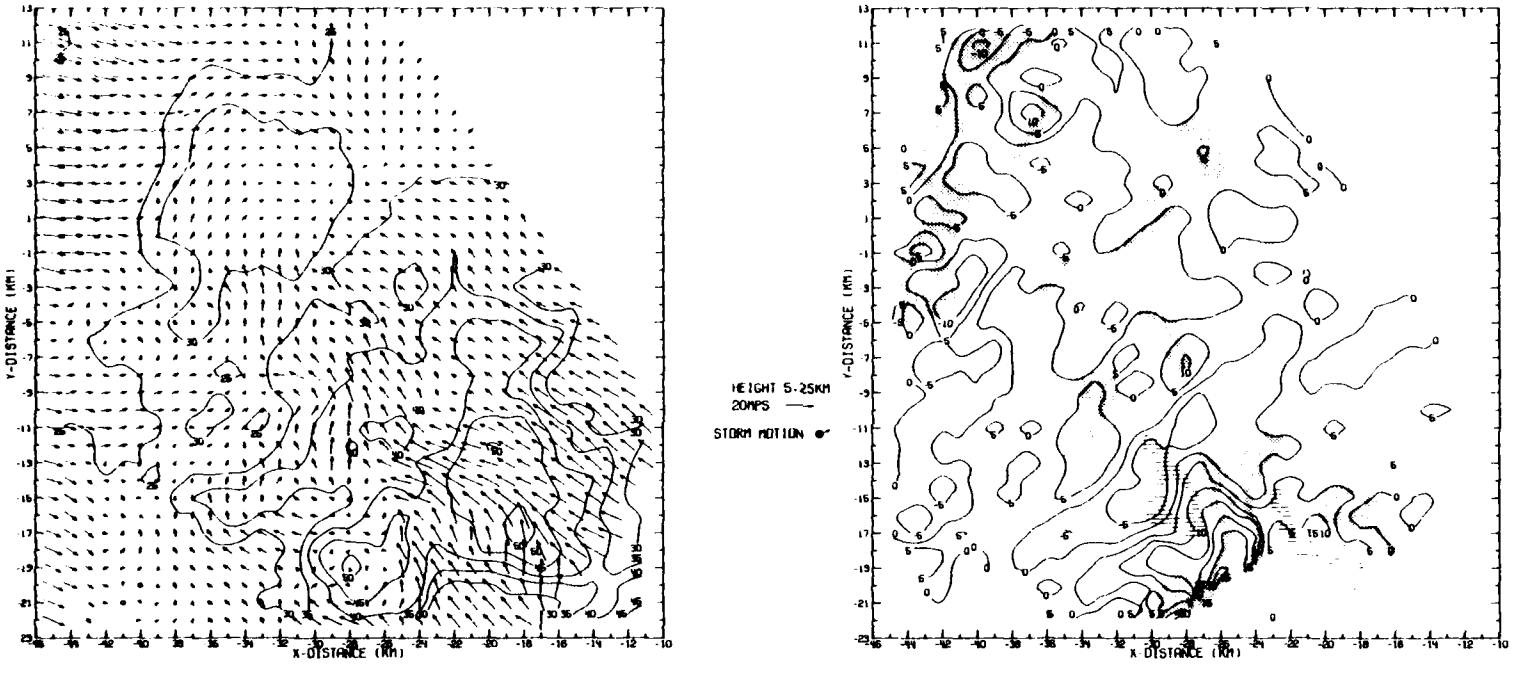

Figure 8. Same as Figure 5 except at a height of 5.25 km.

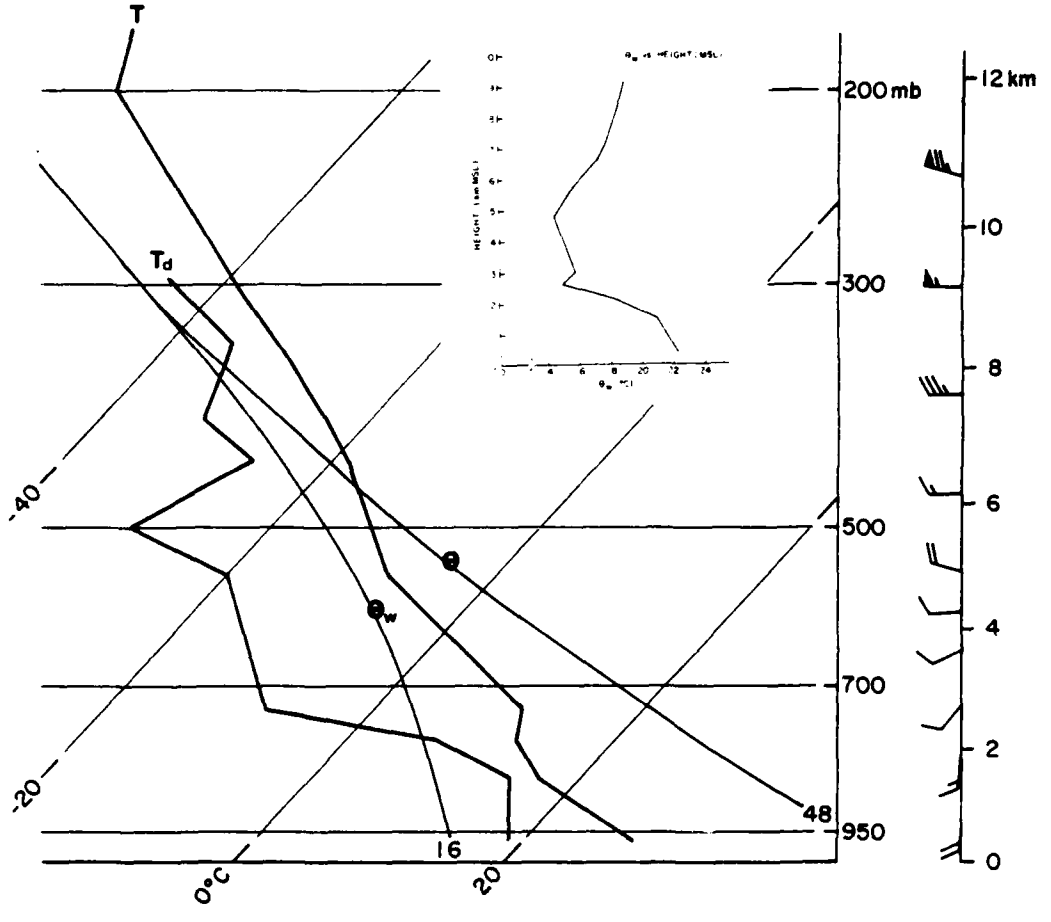

Figure 9. Skew T - log P diagram of the Oklahoma City sounding taken at 1800 CST on 3 May 1977. The mean heights in km MSL are given on the right. The winds are illustrated with a half barb = 2.5 m s^{-1}; full barb = 5 m s^{-1}; and flag = 25 m s^{-1}. The insert is a plot of Θ_w versus the height in km MSL taken from this sounding.

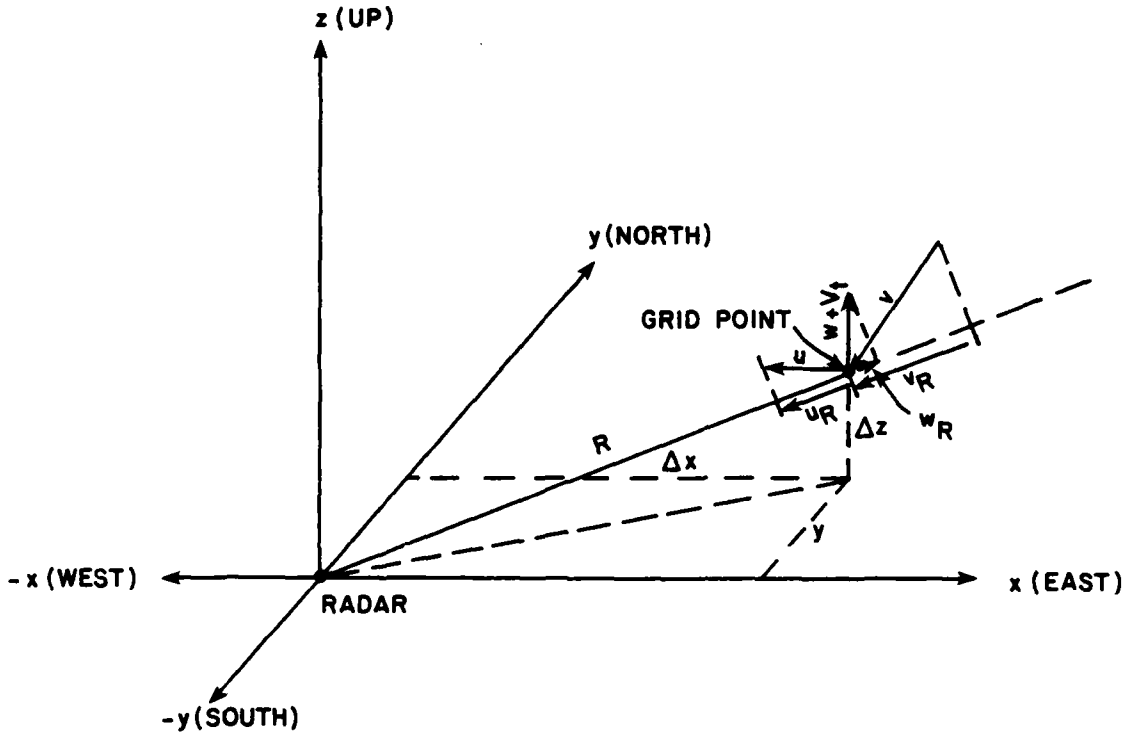

Figure 10. Illustration of conversion back to single-Doppler winds, with u, v, w, and V_t the obtained values from the dual-Doppler analysis. u_R, v_R, and w_R are the radial components of the u, v, and $(w + V_t)$ respectively. R is the distance from the radar to the grid point.

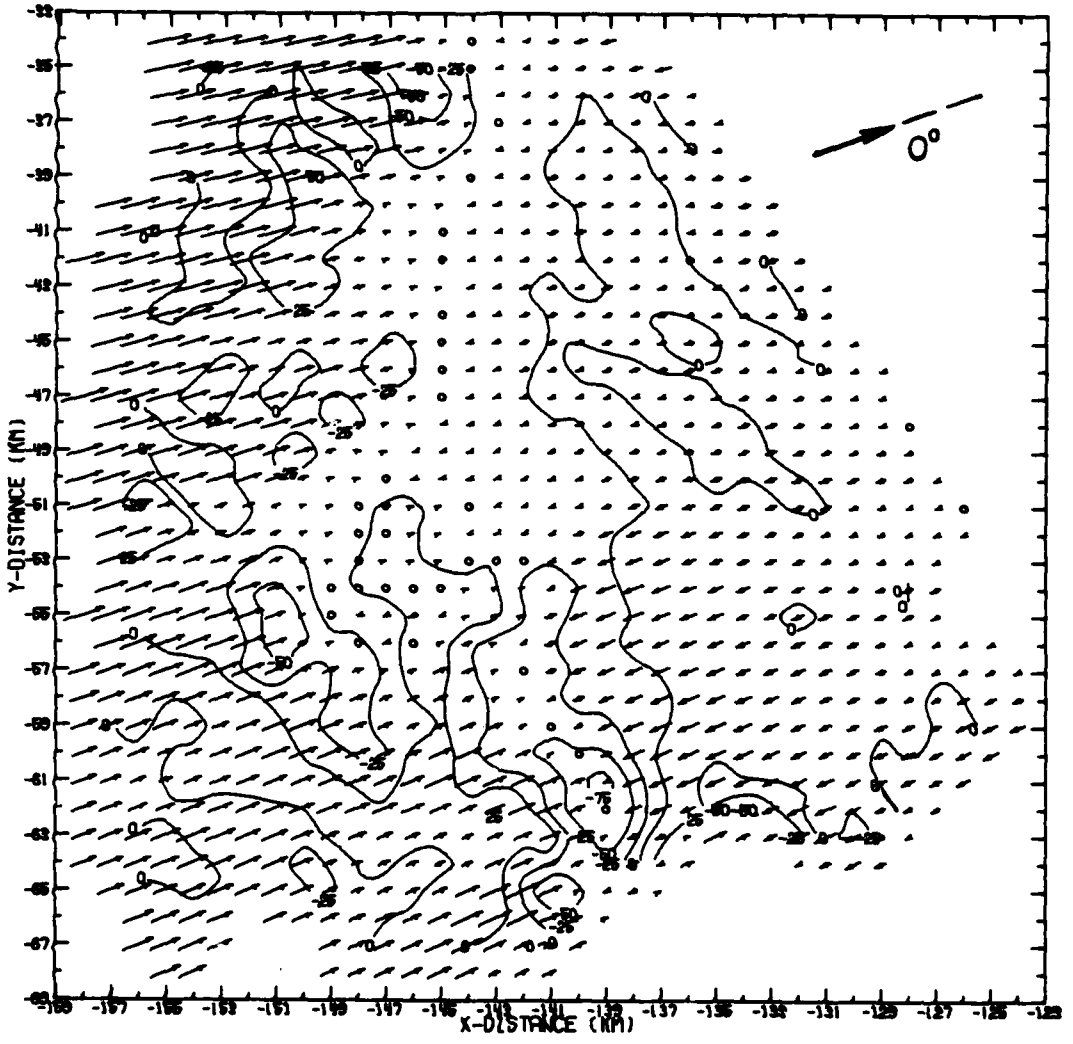

Figure 11. Radial wind field seen from a viewing angle of 0.0°. This is the dual-Doppler wind field converted back to radial winds as would be seen by a fictious Doppler radar located 150 km from the storm. The arrow in the upper right represents the direction of storm motion, with the dashed line representing the orientation of the radar beam. The angle shown is equal to the azimuth of the radar minus the direction of storm motion. Positive X and Y distances are shown in km to the east and north of the radar respectively. Arrows are interpreted as in Figures 5 through 8. Storm motion of 250° at 8.3 m s^{-1} was subtracted from the wind field. Divergence values (x 10^{-4} s^{-1}) are contoured over the wind field.

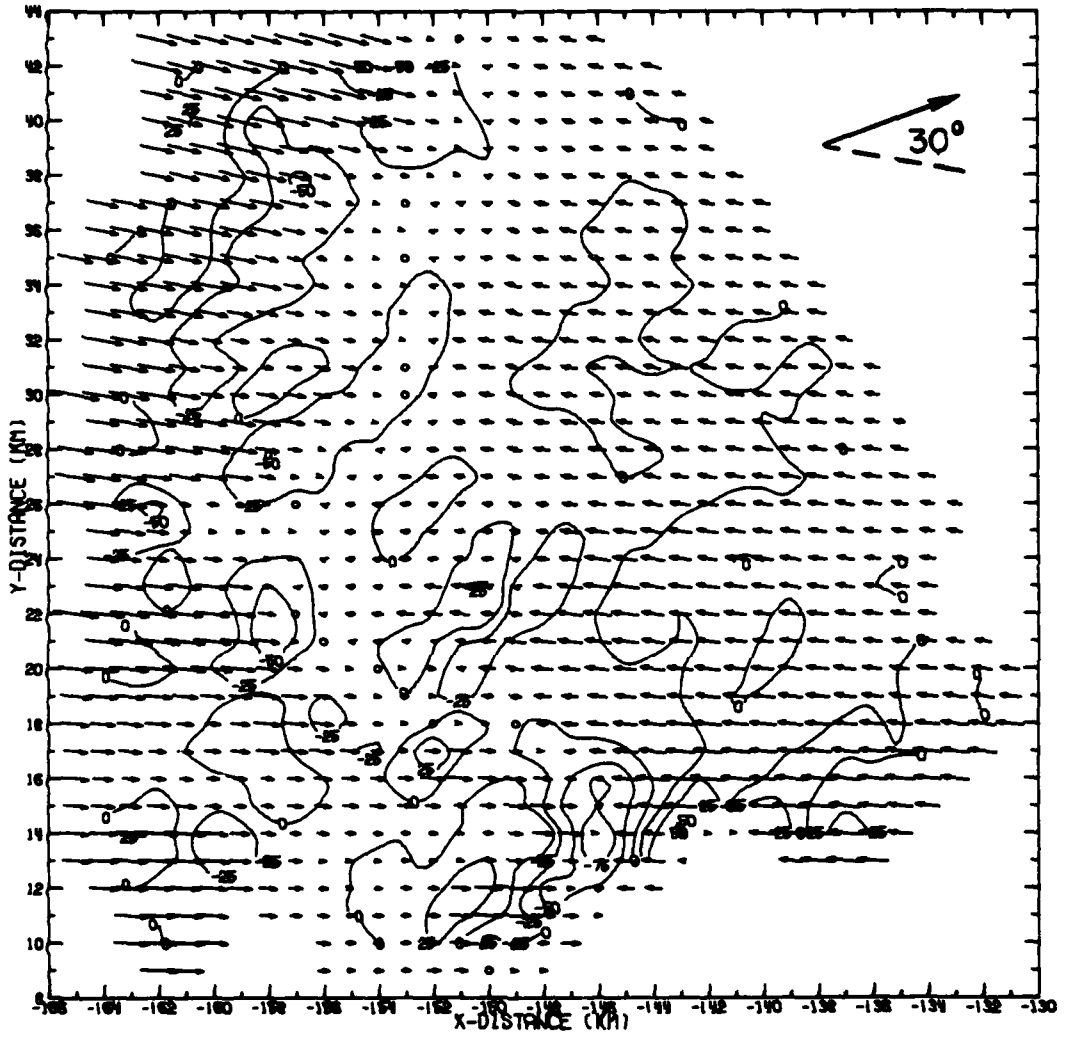

Figure 12. Same as Figure 11 except at a viewing angle of 30°.

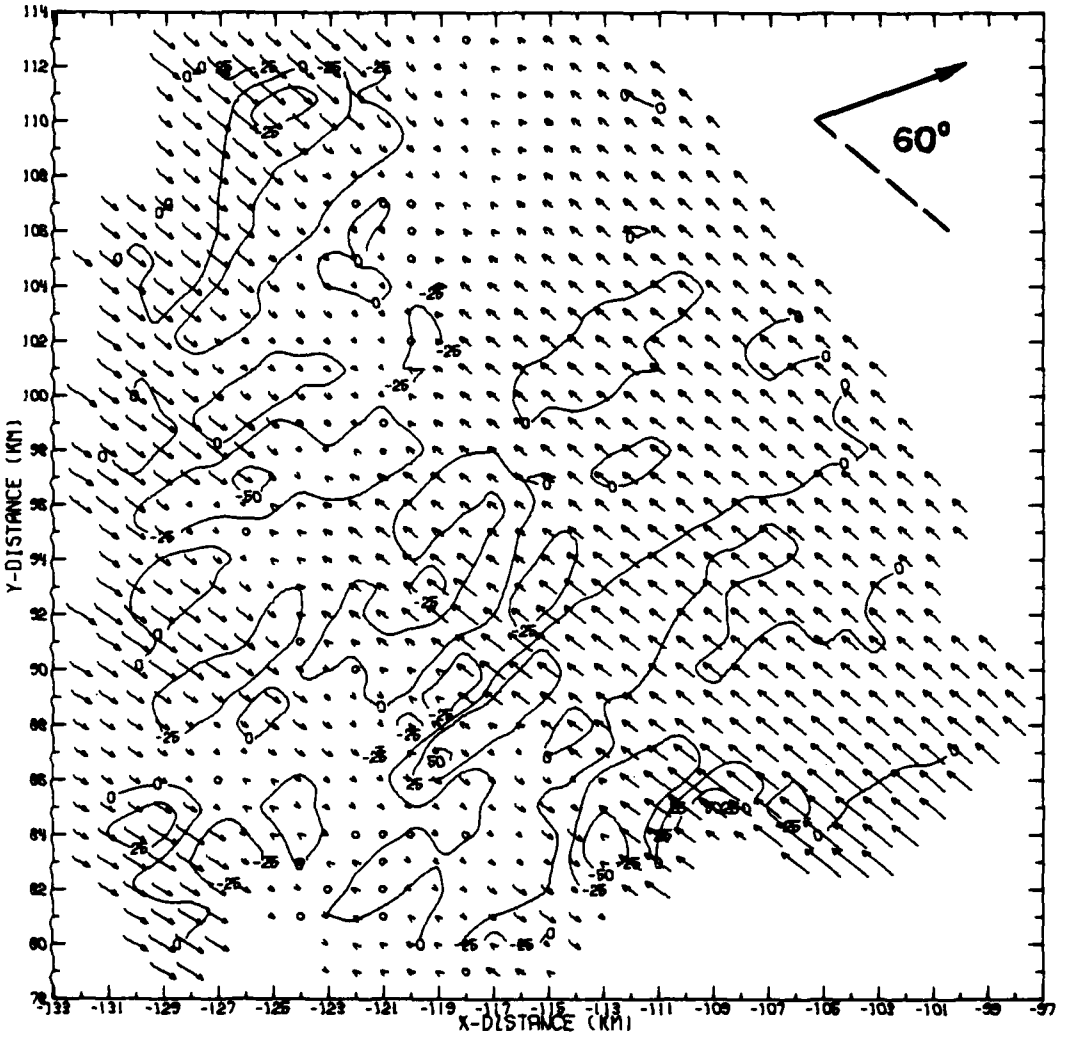

Figure 13. Same as Figure 11 except at a viewing angle of 60°.

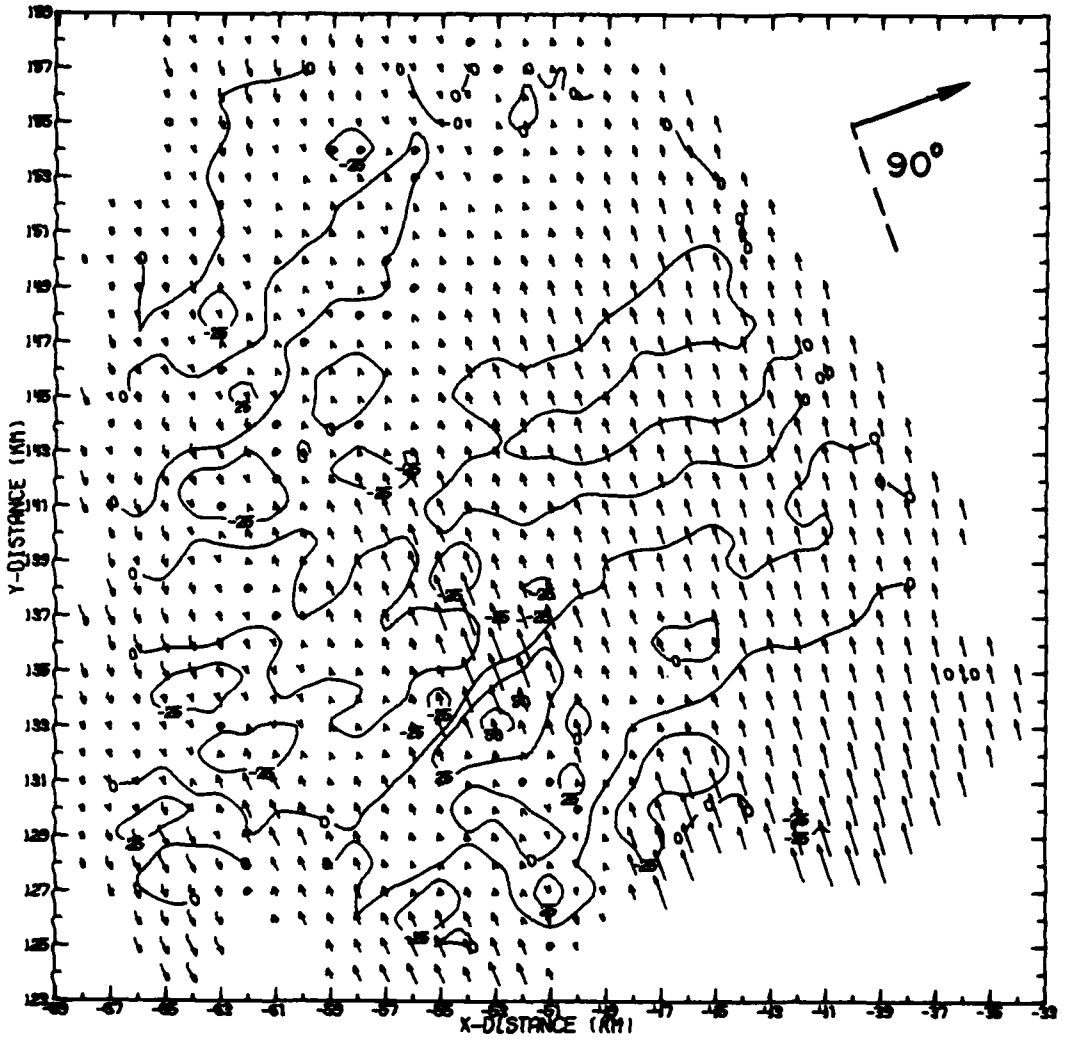

Figure 14. Same as Figure 11 except at a viewing angle of 90°.

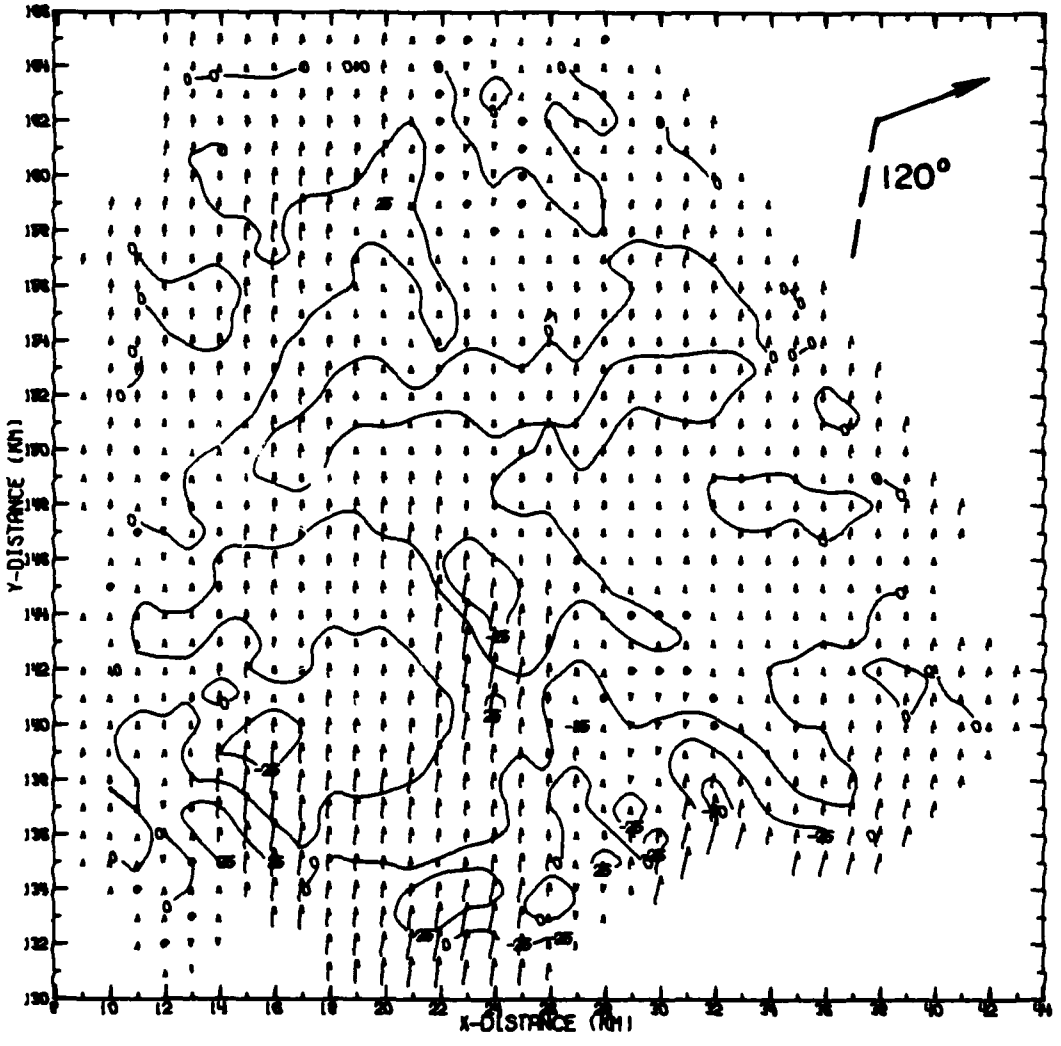

Figure 15. Same as Figure 11 except at a viewing angle of 120°.

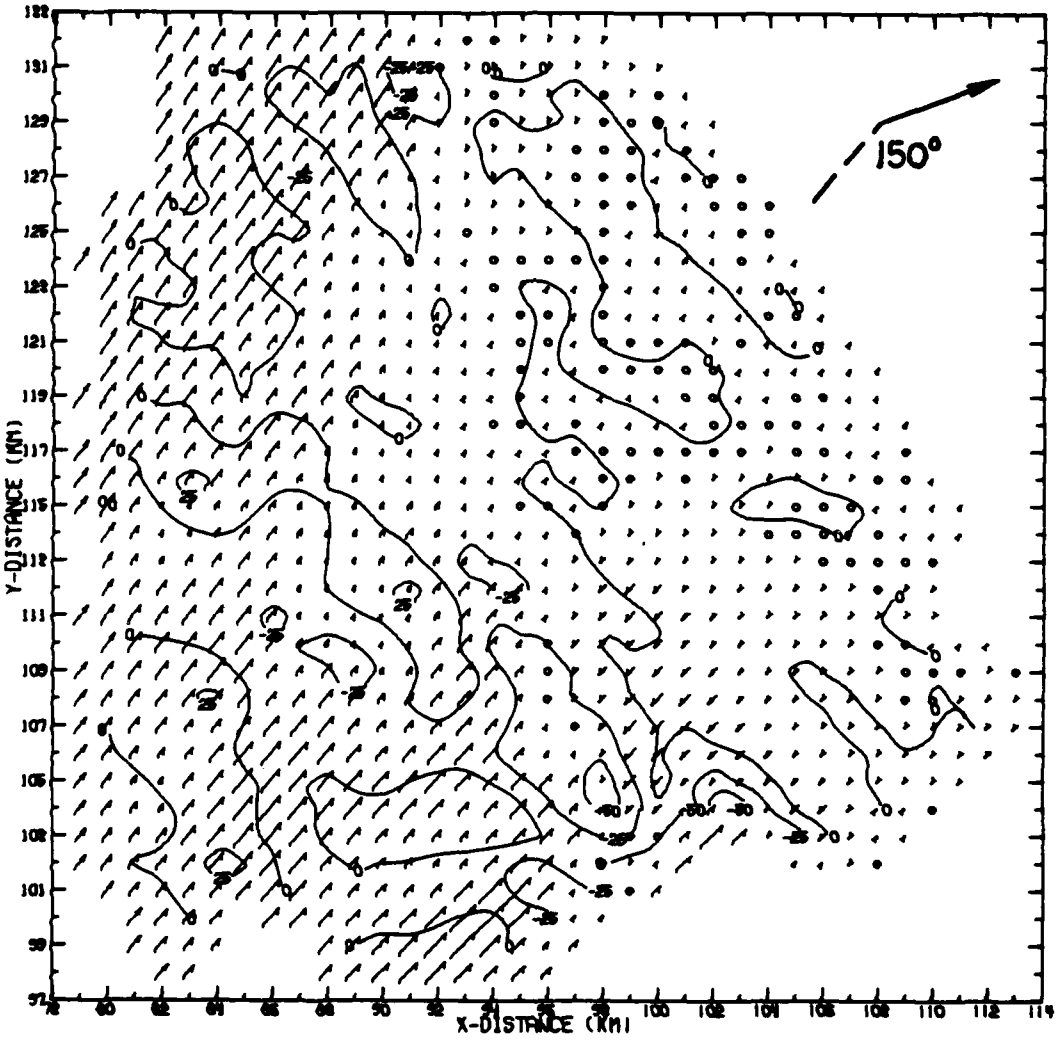

Figure 16. Same as Figure 11 except at a viewing angle of 150°.

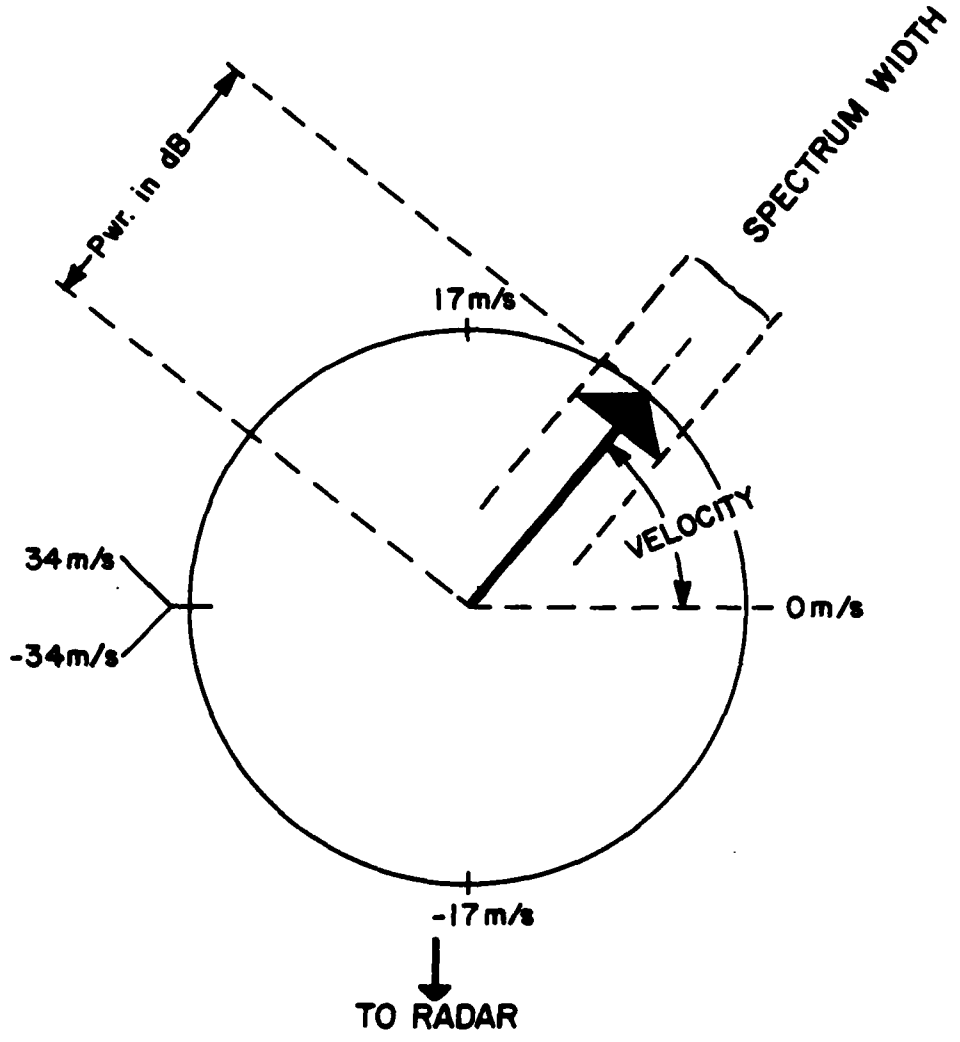

Figure 17. Explanation of multimoment display. Arrow length is proportional to reflectivity, arrow direction to velocity, and arrowhead size to Doppler spectrum width. This is shown with the normal PRF of 1300 Hz or unambiguous velocity interval of ± 34 m s^{-1}. (Burgess et al., 1976)

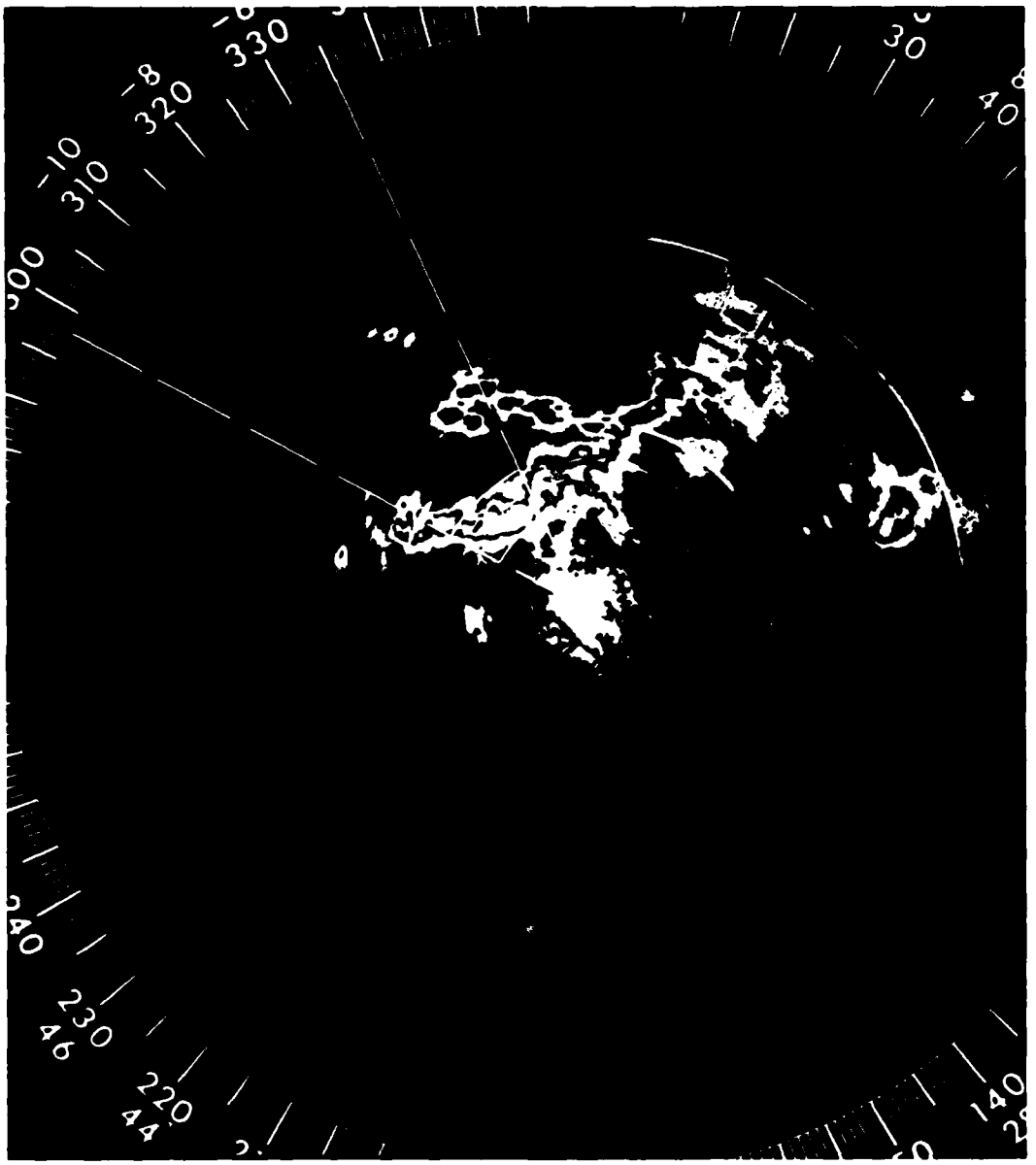

Figure 18. Reflectivity display taken from the Norman WSR-57 at 1205 CST on 21 June 1978, at an elevation angle of 0.0°. The dashed lines show the sector sampled for the multimoment displays shown in Figures 19 and 20. Range circles are at 100 km intervals.

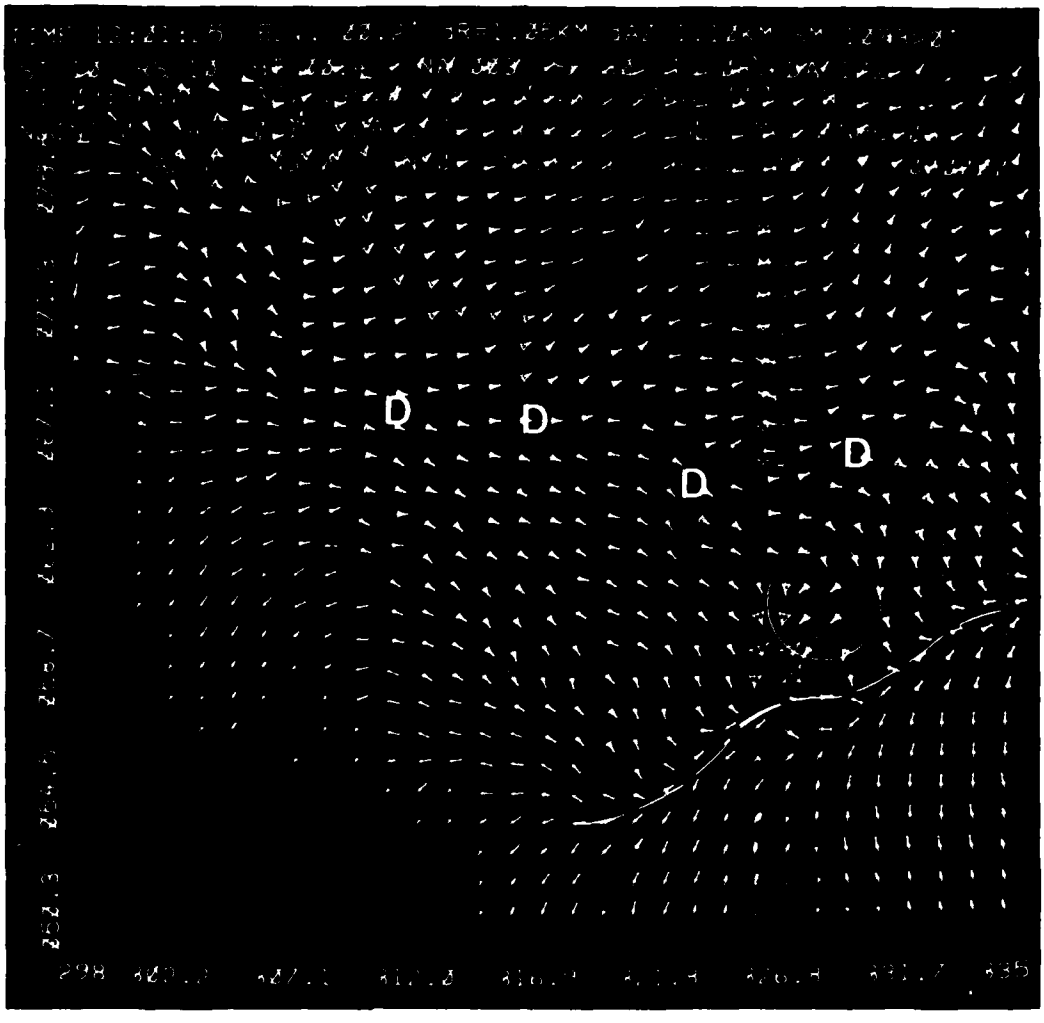

Figure 19. Multimoment display of 21 June 1978 at 1201:25 CST. The top of the figure shows information about the data displayed. Time is as shown in CST. ELV is the elevation angle (0.2°). The distance, in km, between data points along a radial (dR) and between radials (daZ) are 1.05 and 1.10 km respectively. SM is the storm motion subtracted from the data (320° at 10 m s^{-1}). HT is the approximate height in km AGL of the center of the display (0.4 km). DA is the Julian date (day 172). The rest of the information is for use by the radar technicians and would furnish little information to the reader for interpreting the display. The azimuth of the radar is shown, in degrees, along the bottom and the distance along the radial (in km) is shown along the left side. The D's show areas of divergent flow. The dashed line shows the estimated location of the gust front. The circle encloses strong outflow winds (≃ 27 m s^{-1}) behind the gust front.

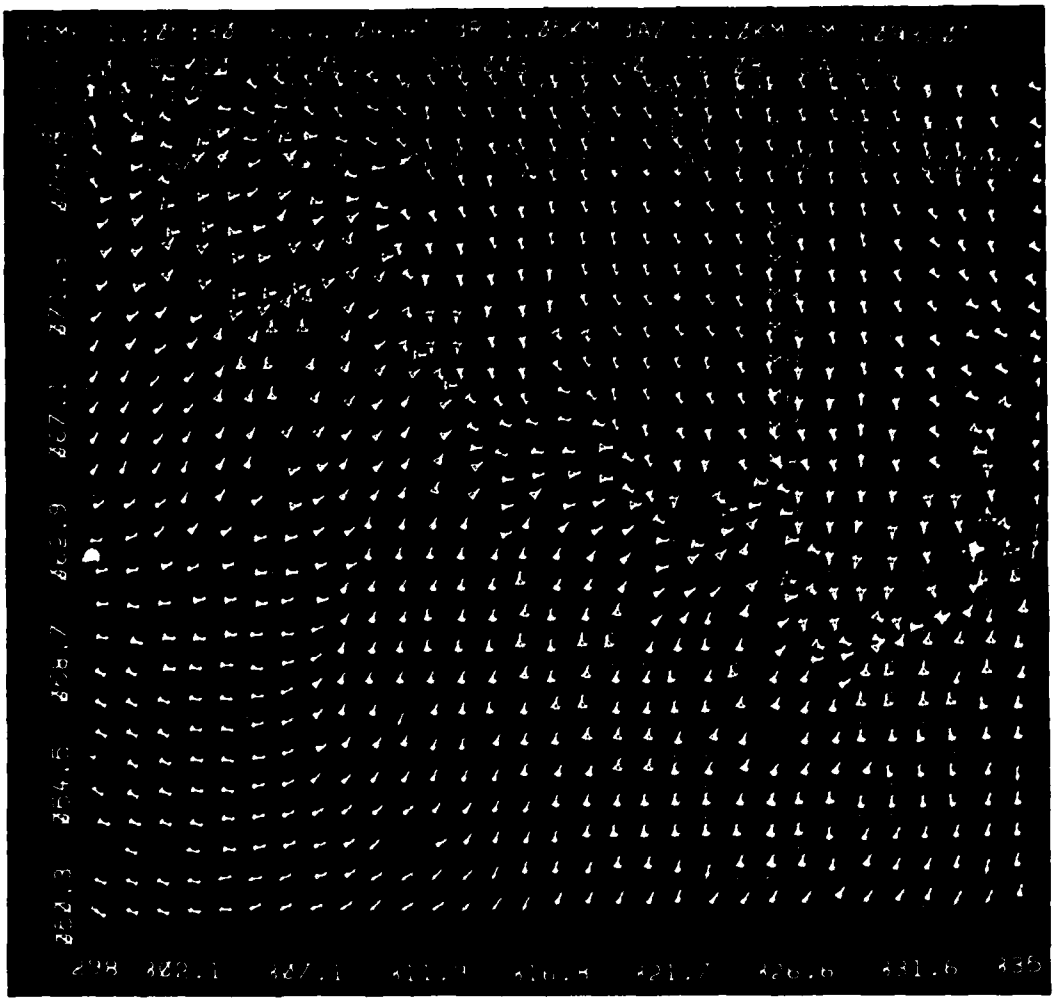

Figure 20. Multimoment display of 21 June 1978 1205:30 CST at an average height of 5.1 km. An explanation of the display is contained in Figures 17 and 19.

Figure 21. Photograph of blowing dust along a gust front on 31 May 1978. The photograph was taken 1 mile south of Anthony, Kansas (Approximately 347° at 190 km from Norman) at 1832 CST. (Photograph taken by John McGinley)

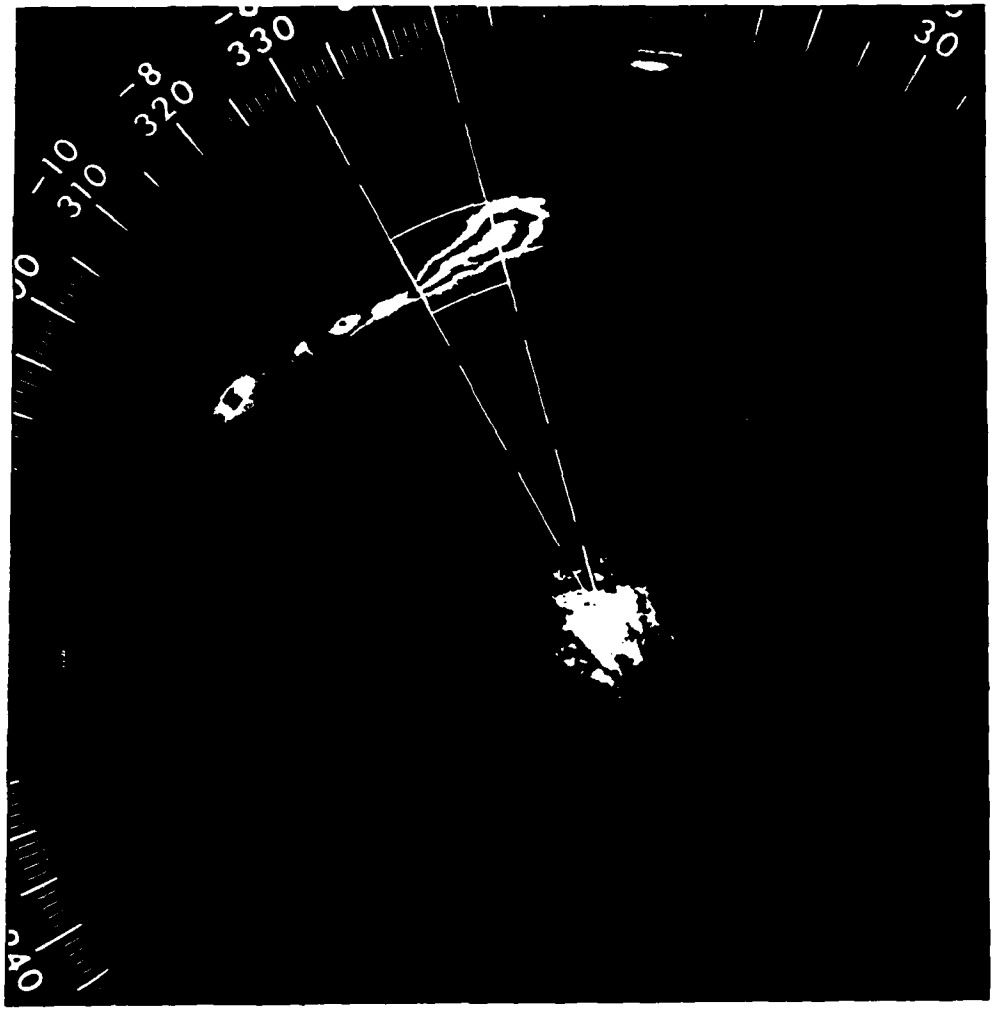

Figure 22. Reflectivity display taken from the Norman WSR-57 at 1822 CST on 31 May 1978. Elevation angle was 0.0°. Range circles are at 100 km intervals. The square illustrates the area shown on the multimoment displays in Figures 23 and 24.

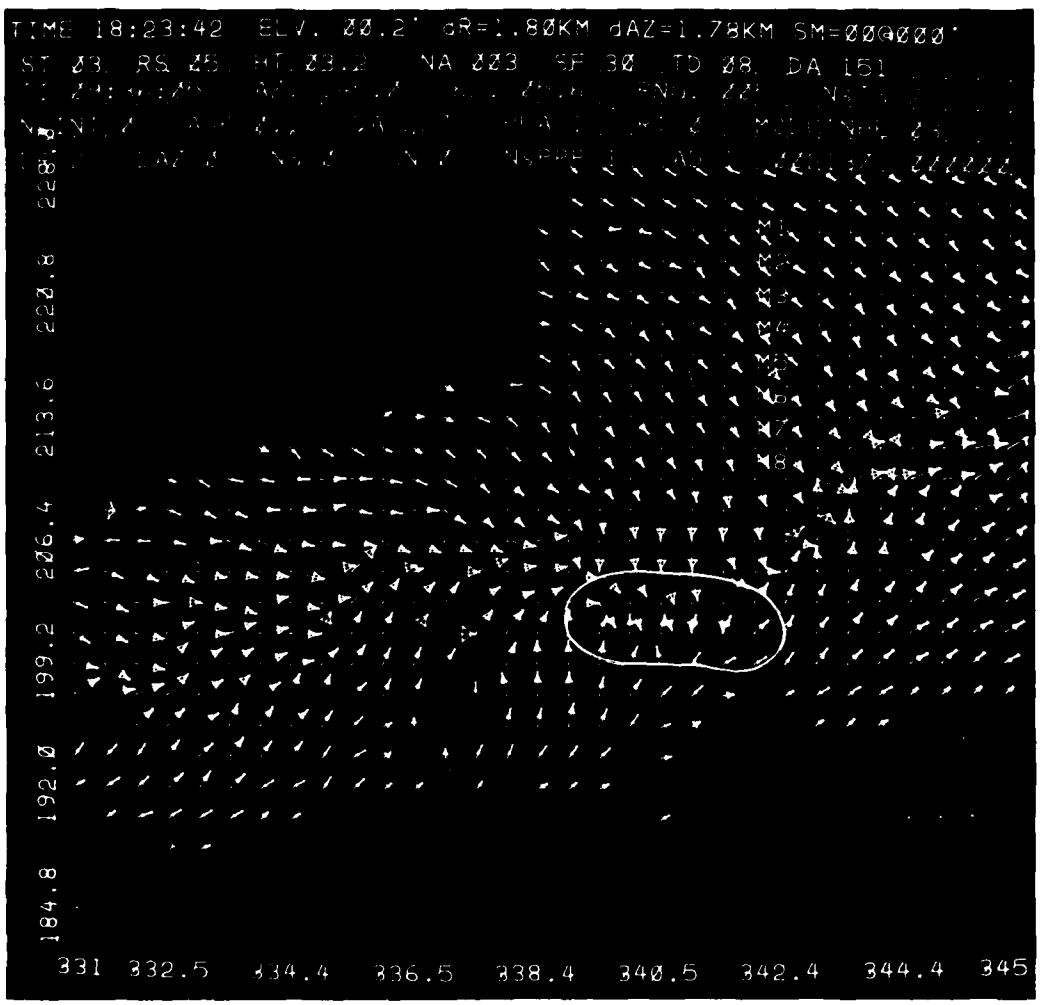

Figure 23. Multimoment display of 31 May 1978 at 1823:42 CST. Elevation angle was 0.2° and the average height was 3.2 km. The area outlined is the area of maximum convergence ($\simeq 1.9 \times 10^{-2}$ s^{-1}). An explanation of the display is contained in Figures 17 and 19.

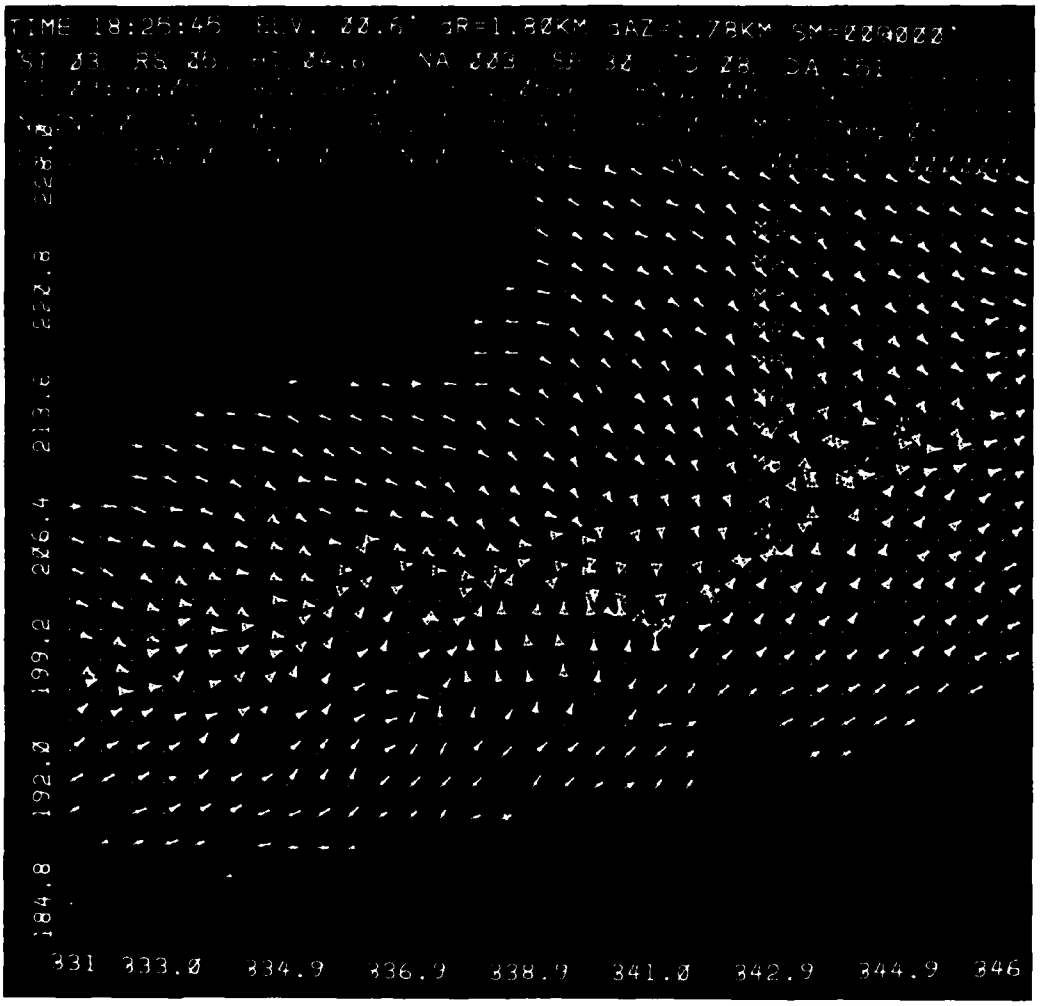

Figure 24. Multimoment display of 31 May 1978 at 1825:45 CST. Elevation angle was 0.6° and the average height was 4.6 km. An explanation of the display is contained in Figures 17 and 19.

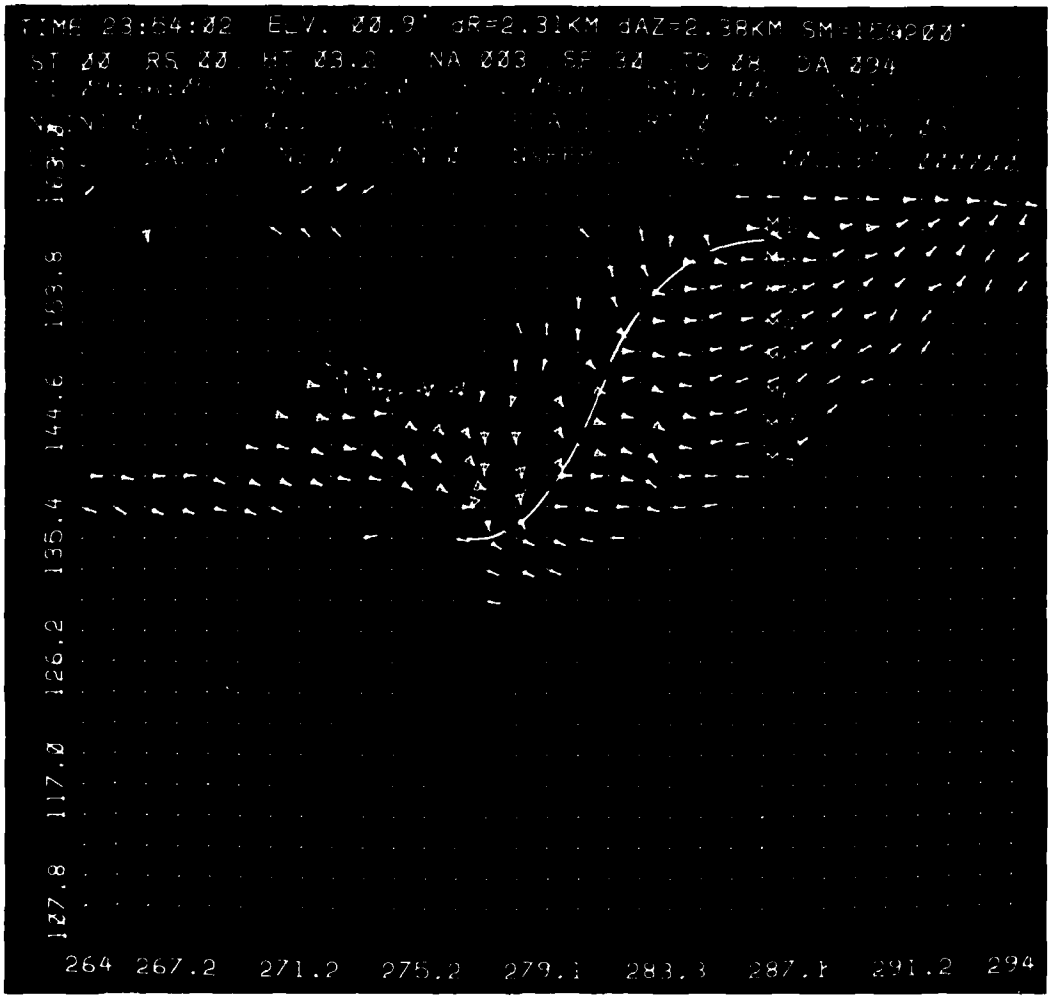

Figure 25. Multimoment display of 4 April 1978 at 2354:02 CST. Elevation angle was 0.9° and the average height was 3.2 km. The PRF during collection was 930 Hz instead of the normal 1300 Hz. Therefore, arrows pointing toward the bottom of the display equal -12 m s^{-1} as opposed to -17 m s^{-1}. The dashed line shows the location of convergence boundary.

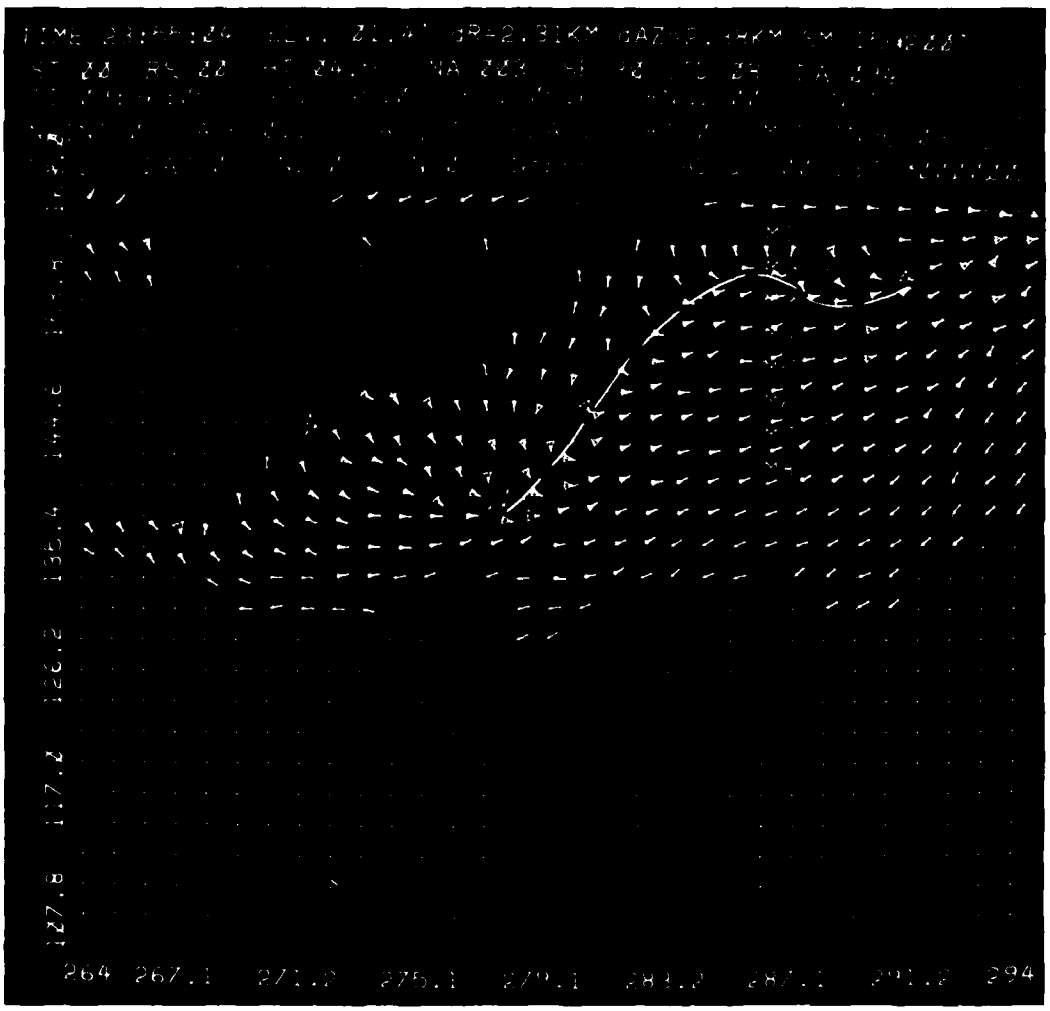

Figure 26. Same as Figure 24 except at 2355:04 CST, elevation angle of 1.4° and average height of 4.5 km.

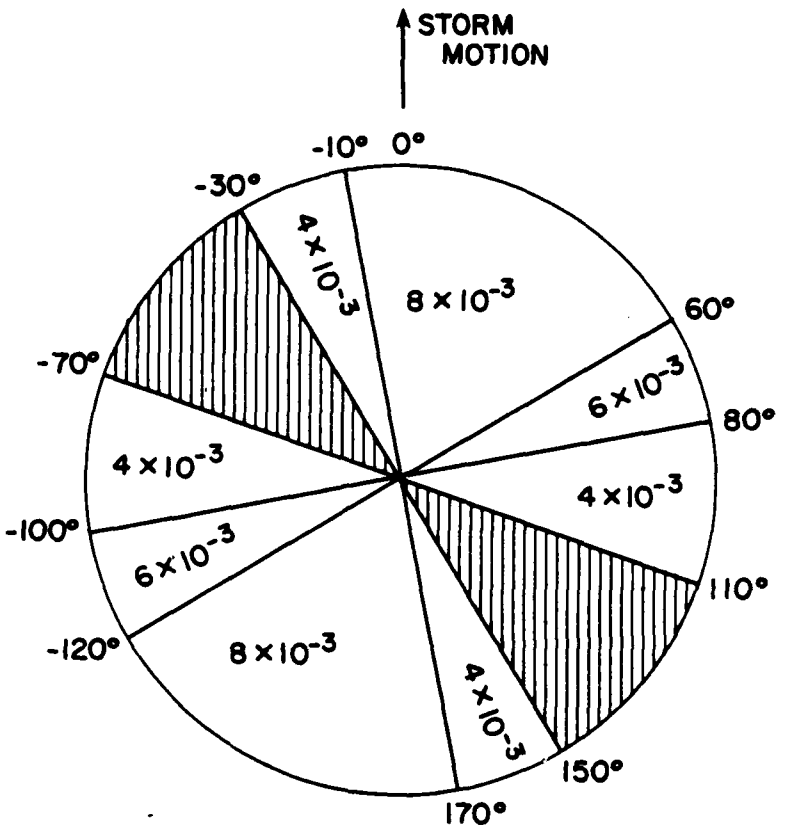

Figure 27. Graph of the proposed minimum convergence (s^{-1}) values (computed along a radial) necessary to produce a downdraft strong enough to result in damaging surface winds ($\geq$ 50 kts) versus the viewing angle of the radar relative to storm motion.

Table 1. Norman and Cimarron Doppler characteristics

	Norman	Cimarron
General		
Wavelength (cm)	10.52	10.94
Peak power (kW)	750	500
Half-power beamwidth (deg.)	0.81	0.85
Pulse length (m)	150	150
Antenna gain (dB)	44.8	43.2
Antenna rotaion rate (deg s^{-1})	6.0	6.0
Reflectivity		
Pulse repetition frequency (Hz)	325	325
Maximum unambiguous range (km)	460	460
Range increment (m)	600	600
Number of data bins per radial	762	762
Intensity resolution	1.3	1.3
Velocity		
Pulse repetition frequency (Hz)	1300^{1}_{2} 1084^{3} 930^{4} 814	1300
Maximum unambiguous velocity (m s^{-1})	$\pm 34.2^{1}_{2}$ 28.5^{3} 24.3^{4} 21.4	±35.6
Range increment (m)	150	150
Maximum unambiguous range (km)	115^{1}_{2} 138^{3} 154^{4} 184	115
Velocity resolution (m s^{-1})	1.08	1.08
Spectral width resolution (m s^{-1})	0.5	0.5

REFERENCES

Armstrong, G.M., and R.J. Donaldson, 1969: Plan shear indicator for real-time Doppler radar identification of hazardous storm winds. J. Appl. Meteor., 8, 376-383.

Barnes, S.L., 1964: A technique for maximizing details in numerical weather map analyses. J. Appl. Meteor., 3, 396-409.

_____, 1978: Oklahoma thunderstorms on 29-30 April 1970. Part I: Morphology of a tornadic storm. Mon. Wea. Rev., 106, 673-684.

Bonewitz, J.D., 1978: Development of Doppler radar techniques for severe thunderstorm wind advisories. Master's Thesis, University of Oklahoma, 69 pp.

Brandes, E.A., 1975: Severe thunderstorm flow characteristics revealed by dual-Doppler observations: 6 June 1974. Preprints, 9th Conf. on Severe Local Storms, Boston, Amer. Meteor. Soc., 85-90.

_____, 1976: Gust front evolution in severe thunderstorms: Preliminary investigation with Doppler radar. Preprints, 7th Conf. on Aerospace and Aeronautical Meteor., Melbourne, Amer. Meteor. Soc., 56-61.

_____, 1977: Gust front evolution and tornado genesis as viewed by Doppler radar. J. Appl. Meteor., 16, 333-338.

Brown, R.A., D.W. Burgess, J.K. Carter, L.R. Lemon, and D. Sirmans, 1975: NSSL dual-Doppler radar measurements in tornadic storms: A preview. Bull. Amer. Meteor. Soc., 56, 524-526.

_____, L.R. Lemon, and D.W. Burgess, 1978: Tornado detection by pulsed Doppler radar. Mon. Wea. Rev., 106, 29-38.

Burgess, D.W., 1976: Single Doppler radar vortex recognition: Part I - Mesocyclone signatures. Preprints, 17th Conf. on Radar Meteor., Boston, Amer. Meteor. Soc., 97-103.

_____, L.D. Hennington, R.J. Doviak, and P.S. Ray, 1976: Multimoment Doppler display for severe storm identification. J. Appl. Meteor., 15, 1302-1306.

Burgess, D.W., J.D. Bonewitz, and D.R. Devore, 1978: Joint Doppler Operational Project: Results year 1. Preprints, 18th Conf. on Radar Meteor., Atlanta, Amer. Meteor. Soc., 442-448.

Byers, H.R., and R.R. Braham, Jr., 1949: The Thunderstorm - A Report of the Thunderstorm Project, U.S. Government Printing Office, 287 pp.

Charba, J., 1972: Gravity current model applied to analysis of squall-line gust front. NOAA Tech. Memo. ERLTM-NSSL No. 61, 58 pp.

_____, 1974: Application of gravity current model to analysis of squall-line gust front. Mon. Wea. Rev., 102, 140-156.

Davies-Jones, R.P., 1979: NSSL Tech. Memo. to be published.

Donaldson, R.J., Jr., 1970: Vortex signature recognition by Doppler radar. J. Appl. Meteor., 9, 661-670.

Fankhauser, J.C., 1971: Thunderstorm-environment interactions determined from aircraft and radar observations. Mon. Wea. Rev., 99, 171-192.

_____, 1976: Structure of an evolving hailstorm, Part III: Thermodynamic structure and airflow in the near environment. Mon. Wea. Rev., 104, 576-587.

Foote, G.B., and P.S. du Toit, 1969: Terminal velocity of raindrops aloft. J. Appl. Meteor., 8, 249-253.

Fujita, T., and F. Caracena, 1977: An analysis of three weather-related aircraft accidents. Bull. Amer. Meteor. Soc., 58, 1164-1181.

Goff, R.C., 1976: Vertical structure of thunderstorm outflow. Mon. Wea. Rev., 104, 1430-1440.

_____, J.T. Lee, and E.A. Brandes, 1977: Gust front analytical study. Report No. FAA-RD-77-119, 140 pp.

JDOP Staff, 1979: Final Report on the Joint Doppler Operational Project (JDOP) 1976-78. NOAA Tech. Memo. ERL-NSSL No. __, __ pp (In press).

Kropfli, R.A., and L.J. Miller, 1975a: Thunderstorm flow patterns in three dimensions. Mon. Wea. Rev., 103, 70-71.

_____, and L.J. Miller, 1975b: Kinematic structure and flux quantities in a convective storm from dual-Doppler radar observations. J. Appl. Meteor., 33, 520-529.

Lemon, L.R., 1977: New severe thunderstorm radar identification techniques and warning criteria. NOAA Tech. Memo. NWS NSSFC-1, 60 pp.

Lemon, L.R., R.J. Donaldson, Jr., D.W. Burgess, and R.A. Brown, 1977: Doppler radar application to severe thunderstorm study and potential real-time warning. Bull. Amer. Meteor. Soc., 58, 1187-1193.

_____, D.W. Burgess, and R.A. Brown, 1978: Tornadic storm airflow and morphology derived from single-Doppler radar measuements. Mon. Wea. Rev., 106, 48-61.

Mitchell, K.E., and J.B. Hovermale, 1977: A numerical investigation of the severe thunderstorm gust front. Mon. Wea. Rev., 105, 657-675.

NSSL Staff, 1971: The NSSL surface network and observations of hazardous wind gusts. NOAA Tech. Memo. ERLTM-NSSL No. 55, 19 pp.

Ogura, Y., and N.A. Phillips, 1962: Scale analysis of deep and shallow convection in the atmosphere. J. Atmos. Sci., 19, 173-179.

Ray, P.S., R.J. Doviak, G.B. Walker, D. Sirmans, J. Carter, and B. Bumgarner, 1975: Dual-Doppler observation of a tornadic storm. J. Appl. Meteor., 14, 1521-1530.

_____, and K.K. Wagner, 1976: Multiple Doppler radar observations of storms. Geophys. Res. Lett., 3, 189-191.

Rogers, R.R., 1964: An extension of the Z-R relation for Doppler radar. Preprints, 11th Weather Radar Conf., Boulder, Colo., Amer. Meteor. Soc., 158-161.

Sirmans, D., and B. Bumgarner, 1975: Numerical comparison of five mean frequency estimators. J. Appl. Meteor., 14, 991-1003.

Walters, G.W., 1975: Severe thunderstorm wind gusts. Master's Thesis, Colorado State University, 81 pp.

END

DATE
FILMED

1-82

DTIC